REGION 4A

Infanta River Basin:

DREAM Flood Forecasting and Flood Hazard Mapping

TRAINING CENTER FOR APPLIED GEODESY AND PHOTOGRAMMETRY

2015

Published by the UP Training Center for Applied Geodesy and Photogrammetry (TCAGP)
College of Engineering
University of the Philippines Diliman
Quezon City
1101 PHILIPPINES

This research work is supported by the Department of Science and Technology (DOST) Grants-in-Aid Program and is to be cited as:

UP TCAGP (2015), DREAM Flood Forecasting and Flood Hazard Mapping for Infanta River Basin, Disaster Risk and Exposure Assessment for Mitigation (DREAM) Program, DOST Grants-in-Aid Program, 64 pp.

For questions/queries regarding this report, contact:

Alfredo Mahar Francisco A. Lagmay, PhD.
Project Leader, Flood Modeling Component, DREAM Program
University of the Philippines Diliman
Quezon City, Philippines 1101
Email: amfal2@yahoo.com

Enrico C. Paringit, Dr. Eng.
Program Leader, DREAM Program
University of the Philippines Diliman
Quezon City, Philippines 1101
E-mail: paringit@gmail.com

National Library of the Philippines
ISBN: 978-971-9695-15-8

Table of Contents

List of Figures

List of Figures

List of Tables

List of Equations

List of Abbreviations

ACDP	Acoustic Doppler Current Profiler
AOI	Area of Interest
ARG	Automated Rain Gauge
AWLS	Automated Water Level Sensor
DAC	Data Acquisition Component
DEM	Digital Elevation Model
DOST	Department of Science and Technology
DPC	Data Processing Component
DREAM	Disaster Risk Exposure and Assessment for Mitigation
DTM	Digital Terrain Model
DVC	Data Validation Component
FMC	Flood Modelling Component
GDS	Grid Developer System
HEC-HMS	Hydrologic Engineering Center – Hydrologic Modeling System
LiDAR	Light Detecting and Ranging
PAGASA	Philippine Atmospheric, Geophysical and Astronomical Services Administration
RIDF	Rainfall Intensity Duration Frequency
SCS	Soil Conservation Service
SRTM	Shuttle Radar Topography Mission
UP-TCAGP	UP Training Center for Applied Geodesy and Photogrammetry

Introduction

Introduction

1.1 About the DREAM Program

The UP Training Center for Applied Geodesy and Photogrammetry (UP TCAGP) conducts a research program entitled "Nationwide Disaster Risk and Exposure Assessment for Mitigation (DREAM) Program" funded by the Department of Science and Technology (DOST) Grants-in-Aid Program. The DREAM Program aims to produce detailed, up-to-date, national elevation dataset for 3D flood and hazard mapping to address disaster risk reduction and mitigation in the country.

The DREAM Program consists of four components that operationalize the various stages of implementation. The Data Acquisition Component (DAC) conducts aerial surveys to collect Light Detecting and Ranging (LiDAR) data and aerial images in major river basins and priority areas. The Data Validation Component (DVC) implements ground surveys to validate acquired LiDAR data, along with bathymetric measurements to gather river discharge data. The Data Processing Component (DPC) processes and compiles all data generated by the DAC and DVC. Finally, the Flood Modeling Component (FMC) utilizes compiled data for flood modeling and simulation.

Overall, the target output is a national elevation dataset suitable for 1:5000 scale mapping, with 50 centimeter horizontal and vertical accuracies. These accuracies are achieved through the use of state-of-the-art airborne Light Detection and Ranging (LiDAR) technology and appended with Synthetic-aperture radar (SAR) in some areas. It collects point cloud data at a rate of 100,000 to 500,000 points per second, and is capable of collecting elevation data at a rate of 300 to 400 square kilometers per day, per sensor

1.2 Objectives and Target Outputs

The program aims to achieve the following objectives:

a) To acquire a national elevation and resource dataset at sufficient resolution to produce information necessary to support the different phases of disaster management,
b) To operationalize the development of flood hazard models that would produce updated and detailed flood hazard maps for the major river systems in the country,
c) To develop the capacity to process, produce and analyze various proven and potential thematic map layers from the 3D data useful for government agencies,
d) To transfer product development technologies to government agencies with geospatial information requirements, and,

e) To generate the following outputs
1) flood hazard map
2) digital surface model
3) digital terrain model and
4) orthophotograph.

1.3 General Methodological Framework

The methodology to accomplish the program's expected outputs are subdivided into four (4) major components, as shown in Figure 1. Each component is described in detail in the following section.

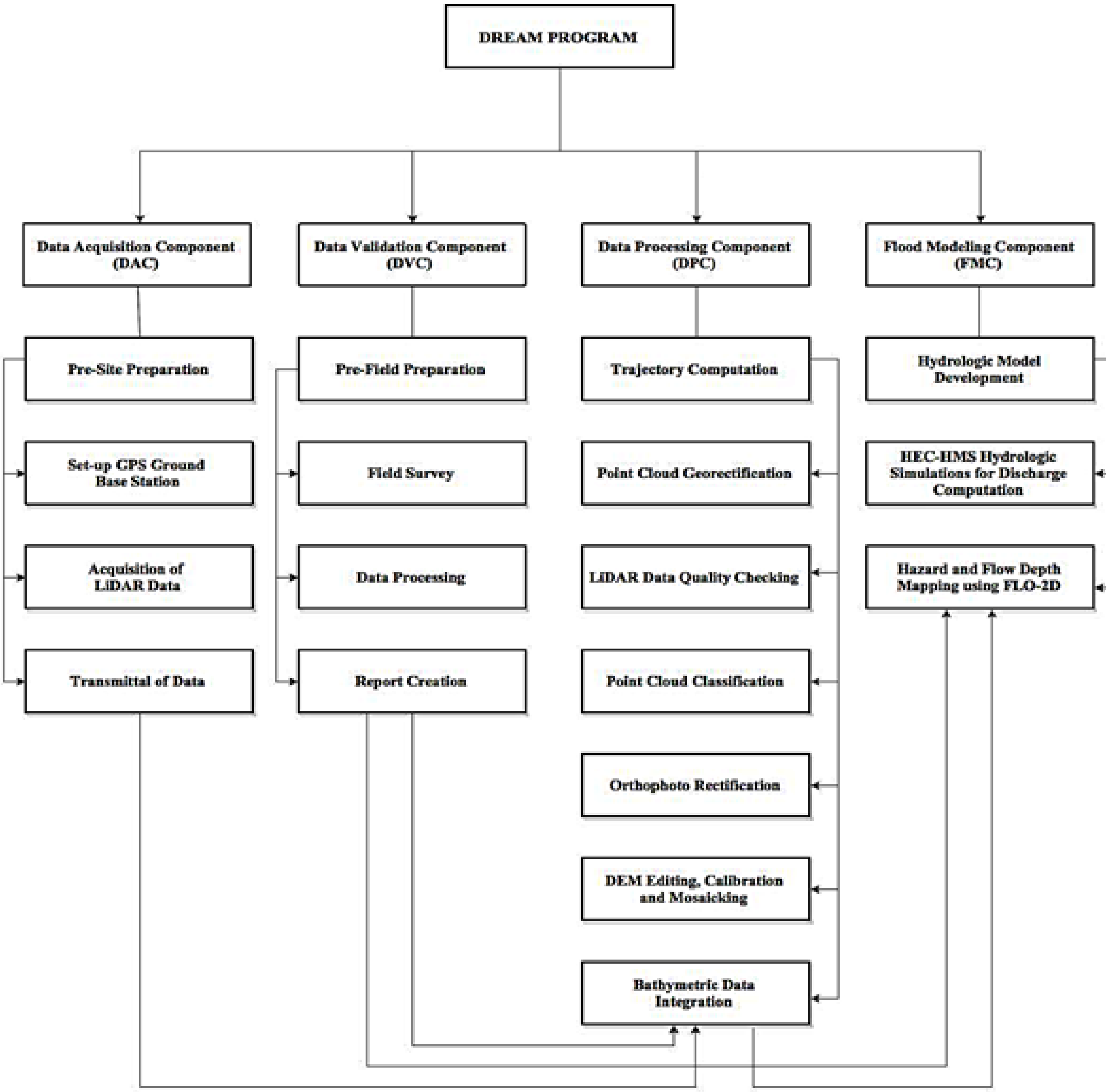

Figure 1. The general methodological framework of the program

1.4 Scope of Work of the Flood Modeling Component

The scope of work of the Flood Modeling Component is listed as the following:

a) To develop the watershed hydrologic model of the Infanta River Basin;
b) To compute the discharge values quantifying the amount of water entering the floodplain using HEC-HMS;
c) To create flood simulations using hydrologic models of the Infanta floodplain using FLO-2D GDS Pro; and
d) To prepare the static flood hazard and flow depth maps for the Infanta river basin.

1.5 Limitations

This research is limited to the usage of the available data, such as the following:

1. Digital Elevation Models (DEM) surveyed by the Data Acquisition Component (DAC) and processed by the Data Processing Component (DPC)
2. Outflow data surveyed by the Data Validation and Bathymetric Component (DVC)
3. Observed Rainfall from ASTI sensors

While the findings of this research could be further used in related-studies, the accuracy of such is dependent on the accuracy of the available data. Also, this research adapts the limitations of the software used: ArcGIS 10.2, HEC-GeoHMS 10.2 extension, WMS 9.1, HEC-HMS 3.5 and FLO-2D GDS Pro.

1.6 Operational Framework

The flow for the operational framework of the Flood Modeling Component is shown in Figure 2.

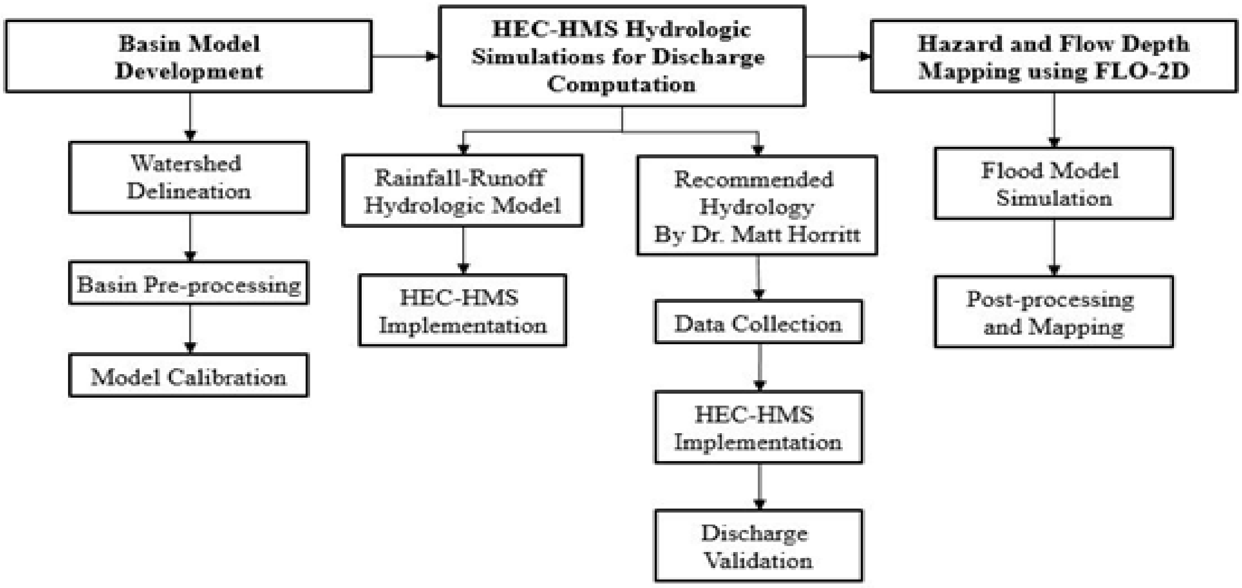

Figure 2. The operational framework and specific work flow of the Flood Modeling Component

The Infanta River Basin

The Infanta River Basin

Infanta River Basin is located in Infanta, province of Quezon. It contains other sub-rivers and the Agos River which separates Infanta from General Nakar, Calabarzon. It covers an area of 1504.35 square kilometers and travels for 8.91 kilometers from its source to its mouth. The location of the Infanta River Basin is as shown in Figure 3.

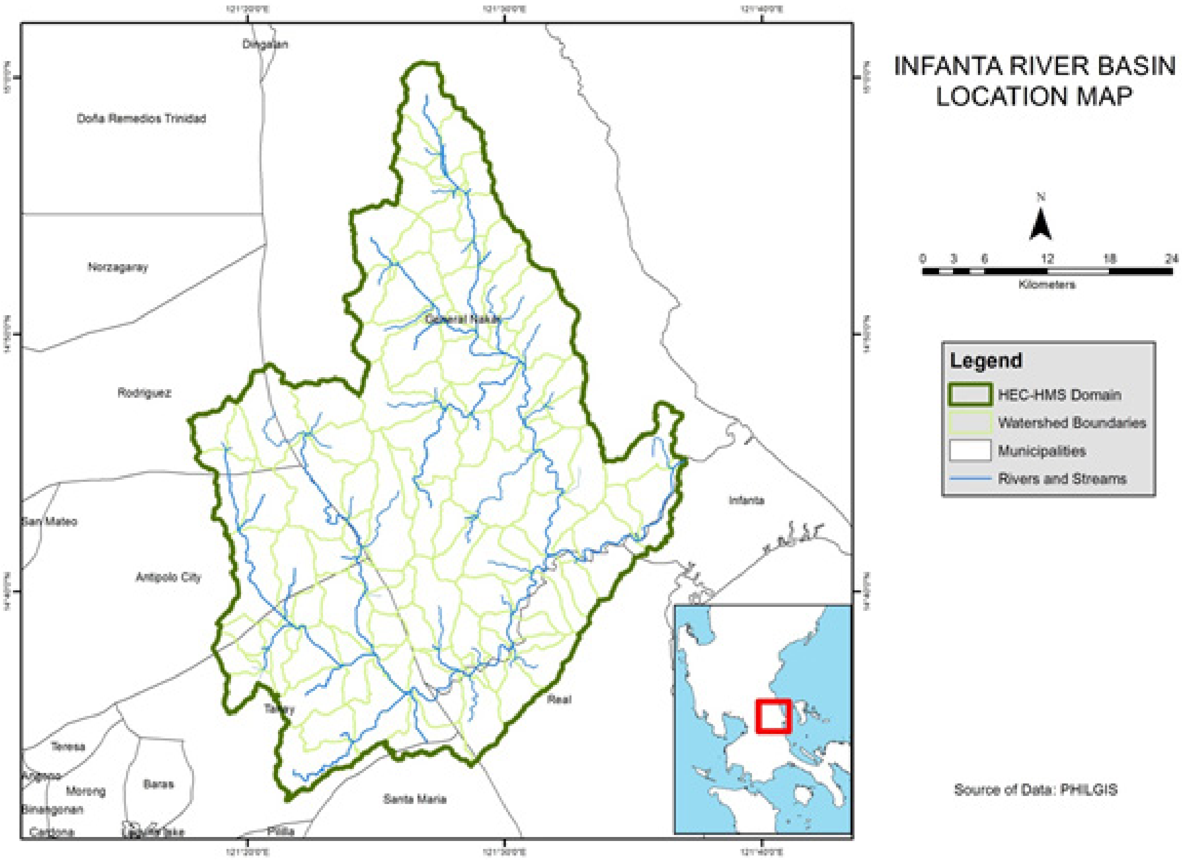

Figure 3. Infanta River Basin Location Map

The land and soil characteristics are important parameters used in assigning the roughness coefficient for different areas within the river basin. The roughness coefficient, also called Manning's coefficient, represents the variable flow of water in different land covers (i.e. rougher, restricted flow within vegetated areas, smoother flow within channels and fluvial environments).

The shape files of the soil and land cover were taken from the Bureau of Soils, which is under the Department of Environment and Natural Resources Management, and National Mapping and Resource Information Authority (NAMRIA). The soil and land cover of Infanta River Basin are shown in Figures 4 and 5, respectively.

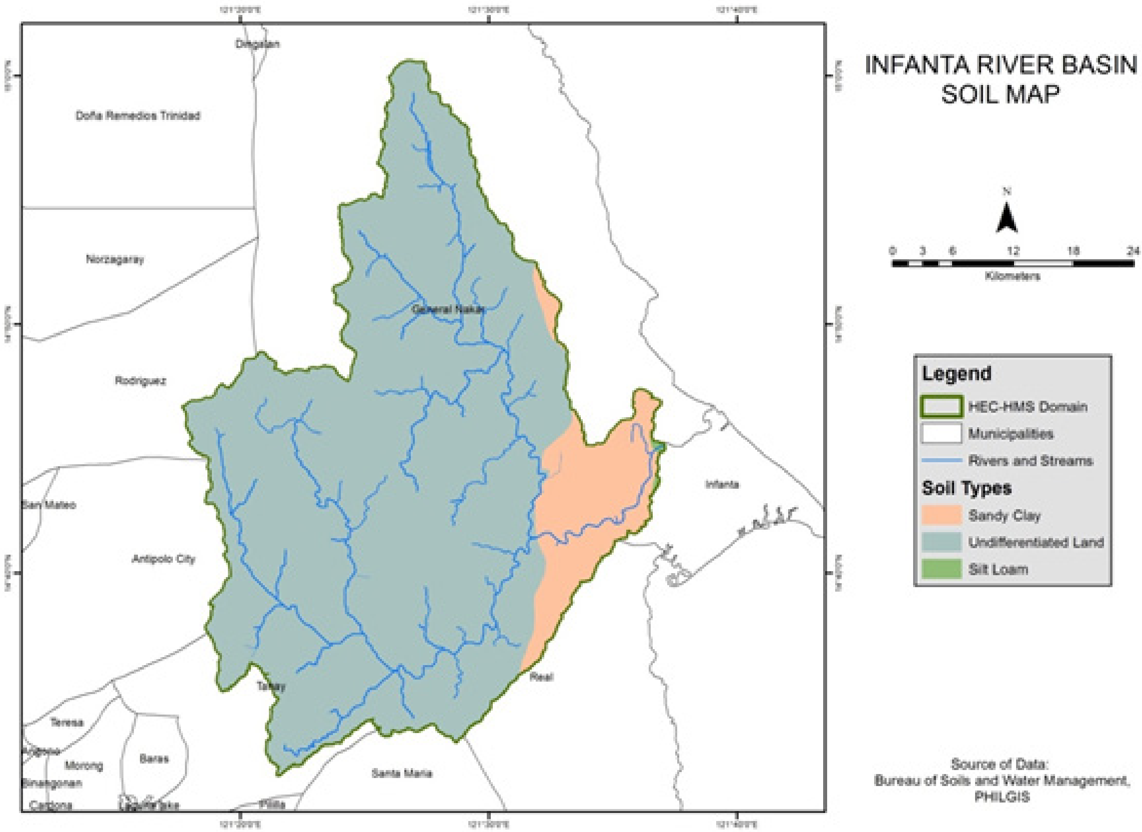

Figure 4. Infanta River Basin Soil Map

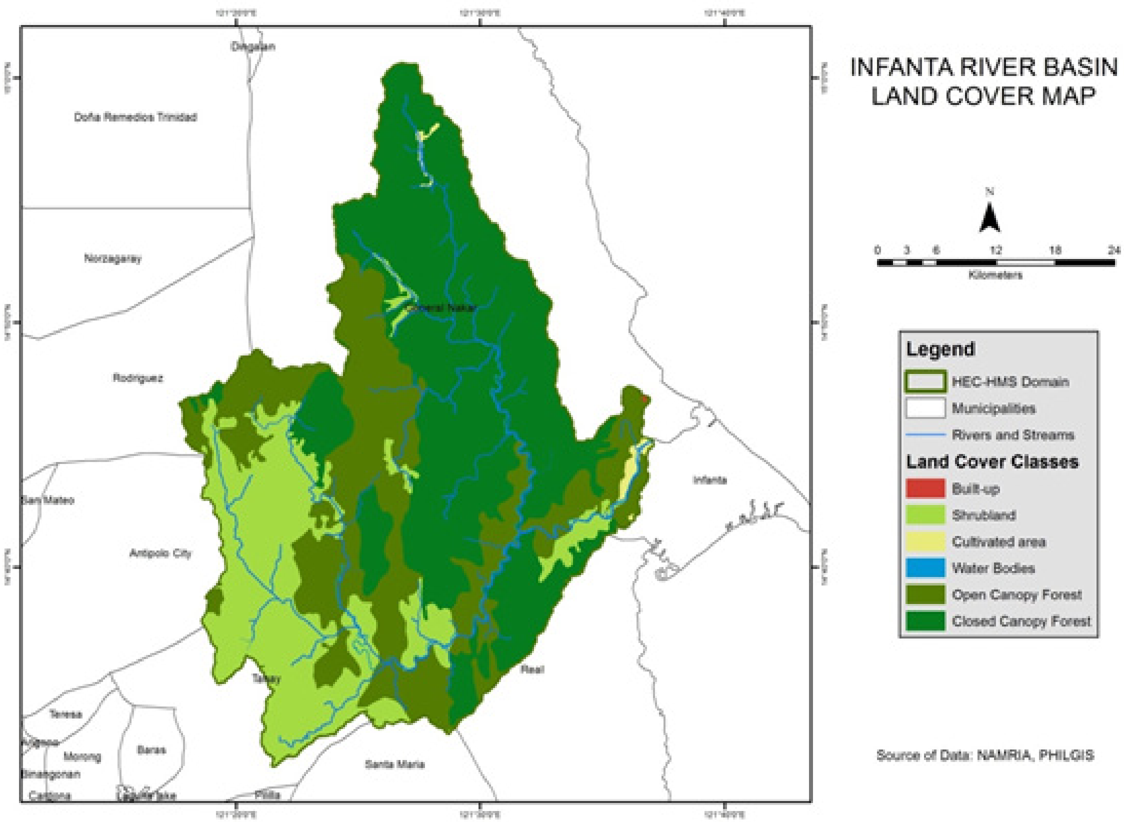

Figure 5. Infanta River Basin Land Cover Map

Methodology

Methodology

3.1 Pre-processing and Data Used

Flood modeling involved several data and parameters to achieve realistic simulations and outputs. Figure 6 shows a summary of the data needed to for the research.

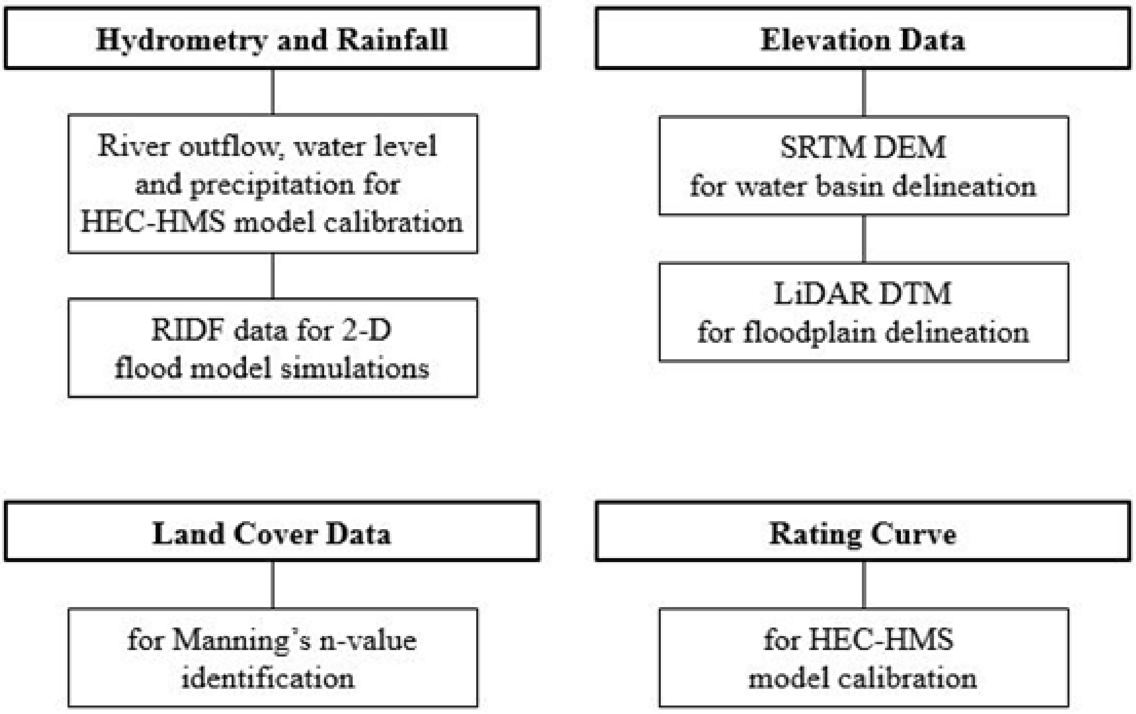

Figure 6. Summary of data needed for the purpose of flood modeling

3.1.1 Elevation Data

3.1.1.1 Hydro Corrected SRTM DEM

With the Shuttle Radar Topography Mission Digital Elevation Model (SRTM DEM) data as an input in determining the extent of the delineated water basin, the model was set-up. The Digital Elevation Model (DEM) is a set of elevation values for a range of points within a designated area. SRTM DEM has a 90 meter spatial mosaic of the entire country. Survey data of cross sections and profile points were integrated to the SRTM DEM for the hydro-correction.

3.1.1.2 LiDAR DEM

LiDAR was used to generate the Digital Elevation Model (DEM) of the different floodplains. DEMs used for flood modeling were already converted to digital terrain models (DTMs) which only show topography, and are thus cleared of land features such as trees and buildings. These terrain features would allow water to flow realistically in the models.

Figure 7 shows an image of the DEM generated through LiDAR.

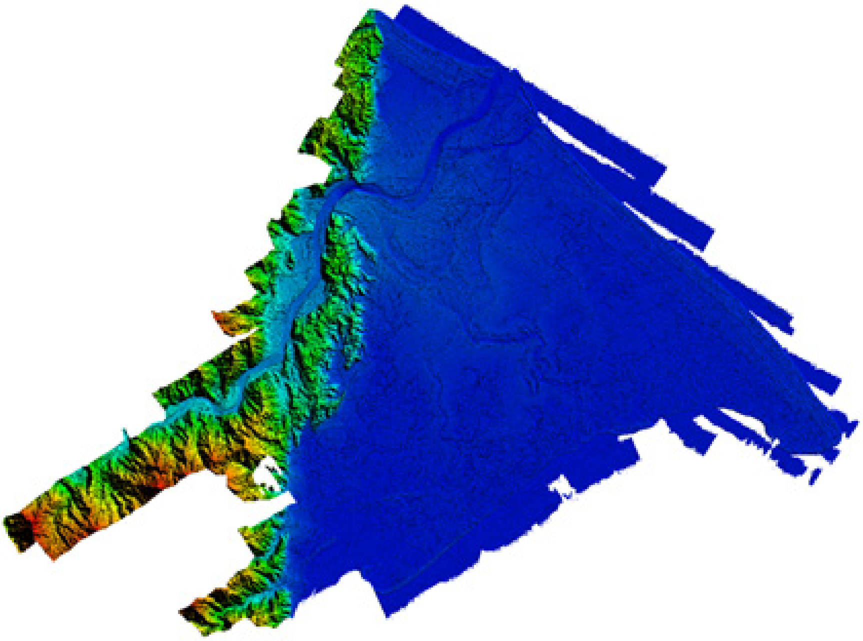

Figure 7. Digital Elevation Model (DEM) of the Infanta River Basin using Light Detection and Ranging (LiDAR) technology

Elevation points were created from LiDAR DTMs. Since DTMs were provided as 1-meter spatial resolution rasters (while flood models for Infanta were created using a 10-meter grid), the DTM raster had to be resampled to a raster grid with a 10-meter cell size using ArcGIS.

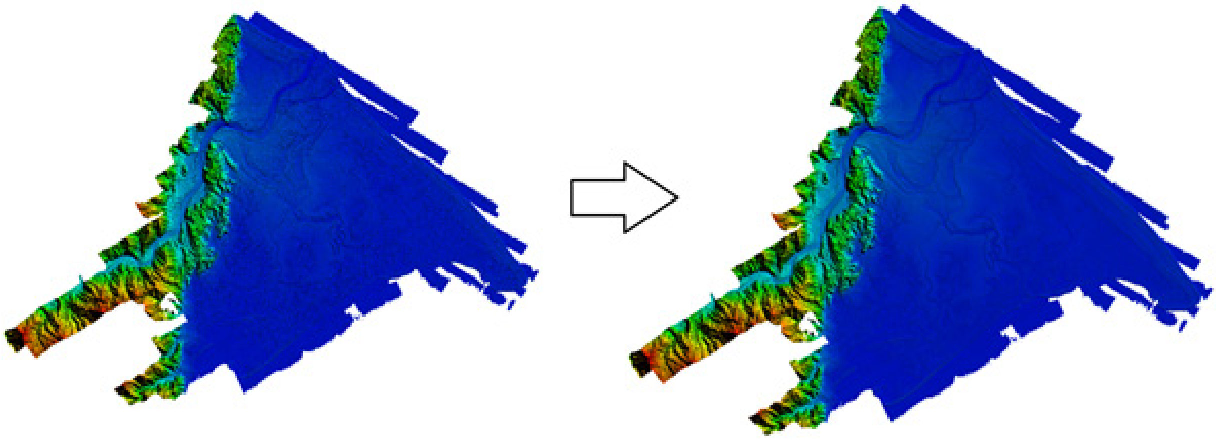

Figure 8. The 1-meter resolution LiDAR data resampled to a 10-meter raster grid in GIS software to ensure that values are properly adjusted

3.1.2 Land Cover and Soil Type

The land and soil characteristics are important parameters used in assigning the roughness coefficient for different areas within the river basin. The roughness coefficient, also called Manning's coefficient, represents the variable flow of water in different land covers (i.e. rougher, restricted flow within vegetated areas, smoother flow within channels and fluvial environments).

A general approach was done for the Infanta floodplain. Streams were identified against built-up areas and rice fields. Identification was done visually using stitched Quickbird images from Google Earth. Areas with different land covers are shown on Figure 9. Different Manning n-values are assigned to each grid element coinciding with these main classifications during the modeling phase.

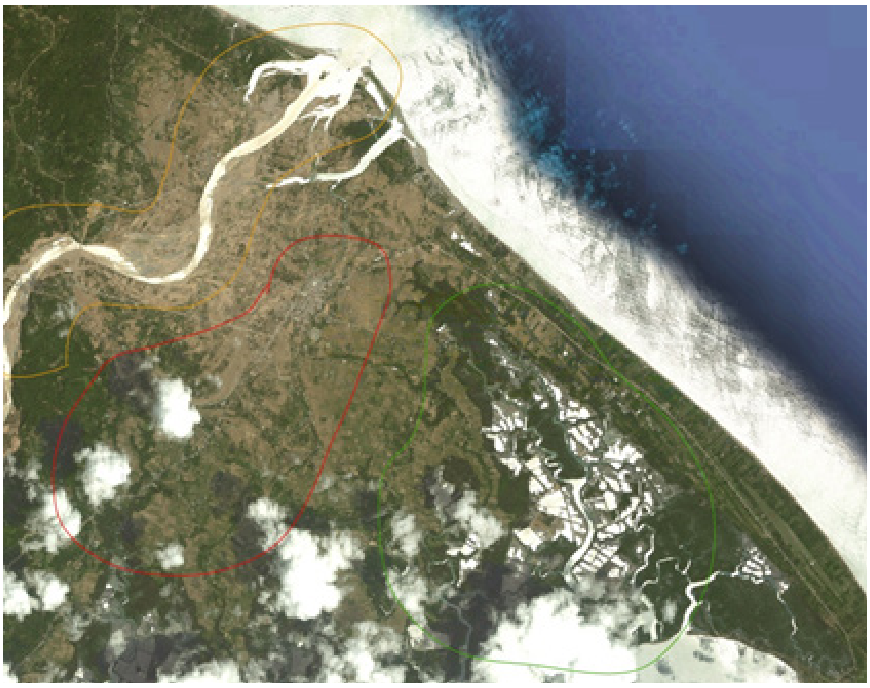

Figure 9. Stitched Quickbird images for the Infanta floodplain

3.1.3 Hydrometry and Rainfall Data

3.1.3.1 Hydrometry for Infanta

The river outflow from Infanta was used to calibrate the HEC-HMS model. This recorded peak discharge is around 10.60cms at 10:05 PM, June 18, 2014.

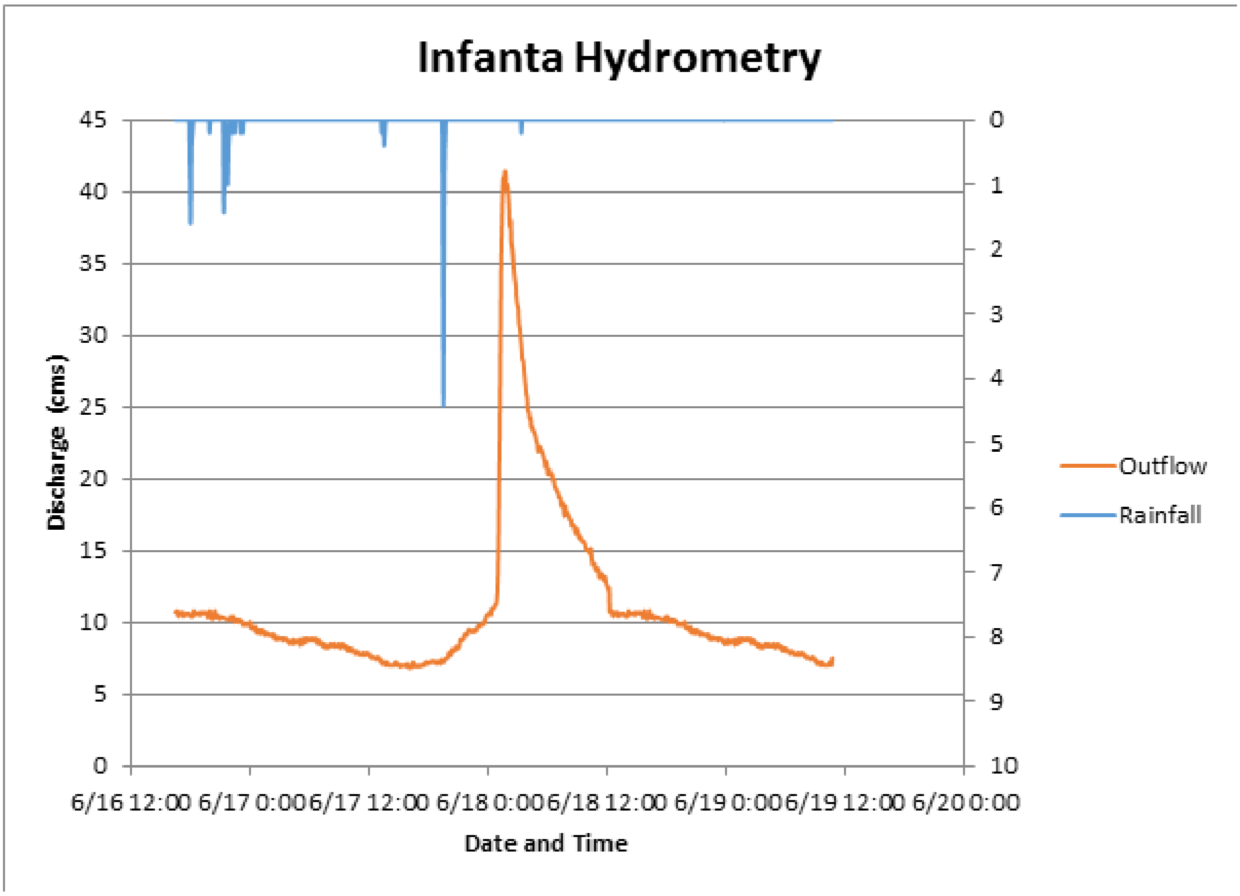

Figure 10. Infanta Rainfall and outflow data used for modeling

3.1.3.2 Rainfall Intensity Duration Frequency

The Philippine Atmospheric Geophysical and Astronomical Services Administration (PAGASA) computed Rainfall Intensity Duration Frequency (RIDF) values for the Infanta Rain Gauge. This station was chosen based on its proximity to the Infanta watershed. The extreme values for this watershed were computed based on a 57-year record.

Five return periods were used, namely, 5-, 10-, 25-, 50-, and 100-year RIDFs. All return periods are 24 hours long and peaks after 12 hours.

Figure 11. Thiessen Polygon of Rain Intensity Duration Frequency (RIDF) Stations for the whole Philippines

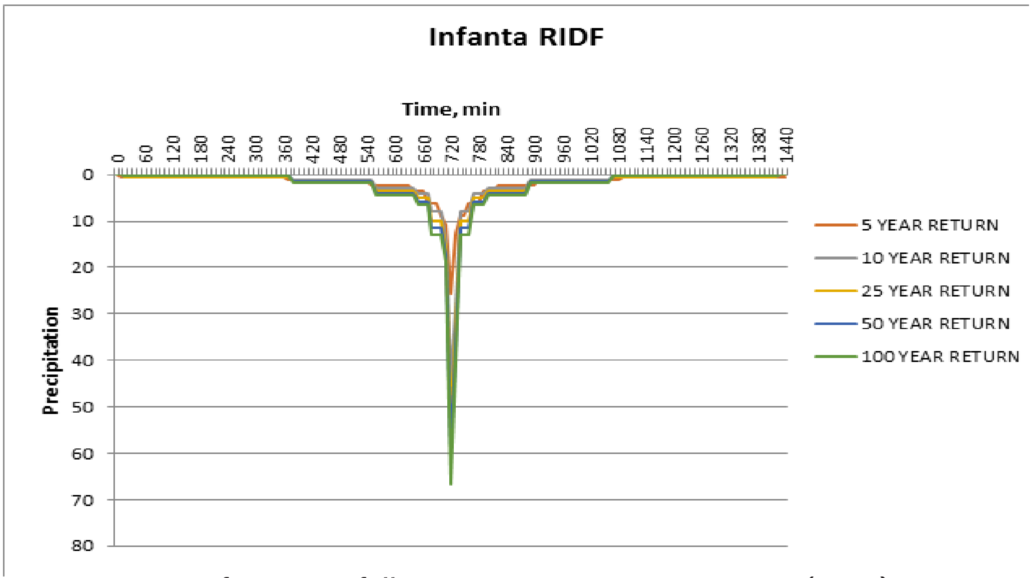

Figure 12. Infanta Rainfall-Intensity Duration Frequency (RIDF) curves

The outflow values at the discharge points in the Infanta river basin were computed for the five return periods, namely, 5-, 10-, 25-, 50-, and 100-year RIDFs.

3.1.4 Rating Curves

Rating curves were provided by DVC. This curve gives the relationship between the observed water levels from the AWLS used and outflow watershed at the said locations.

Rating curves are expressed in the form of Equation 1 with the discharge (Q) as a function of the gauge height (h) readings from the AWLS and constants (a and n).

$$Q = a^{nh}$$

Equation 1. Rating Curve

For Infanta, the rating curve is expressed as $Q = 8E\text{-}19e^{1.0267h}$ as shown in Figure 13.

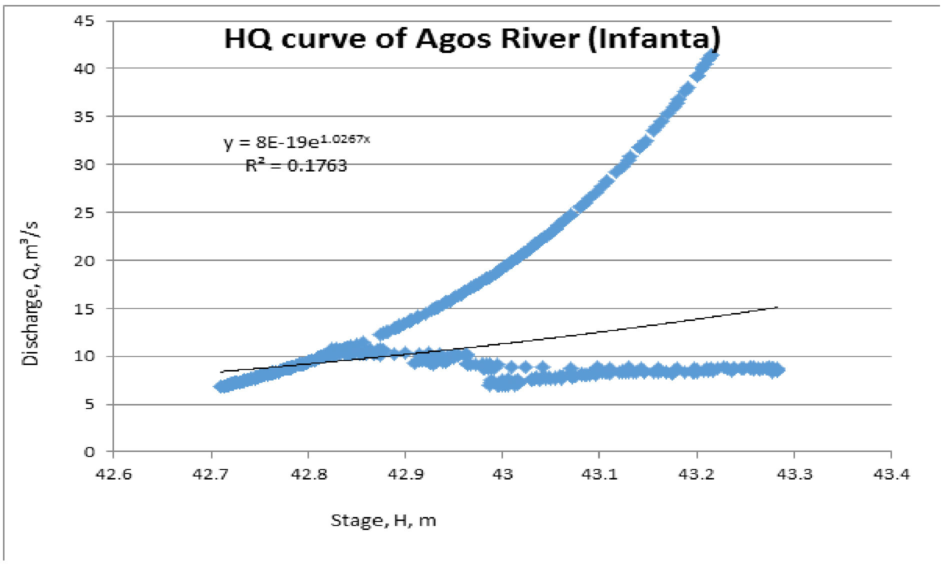

Figure 13. Water level vs. Discharge Curve for Infanta

3.2 Rainfall-Runoff Hydrologic Model Development

3.2.1 Watershed Delineation and Basin Model Pre-processing

The hydrologic model of Infanta River Basin was developed using Watershed Modeling System (WMS) version 9.1. The software was developed by Aquaveo, a water resources engineering consulting firm in United States. WMS is a program capable of various watershed computations and hydrologic simulations. The hydrologic model development follows the scheme shown in the Figure 14.

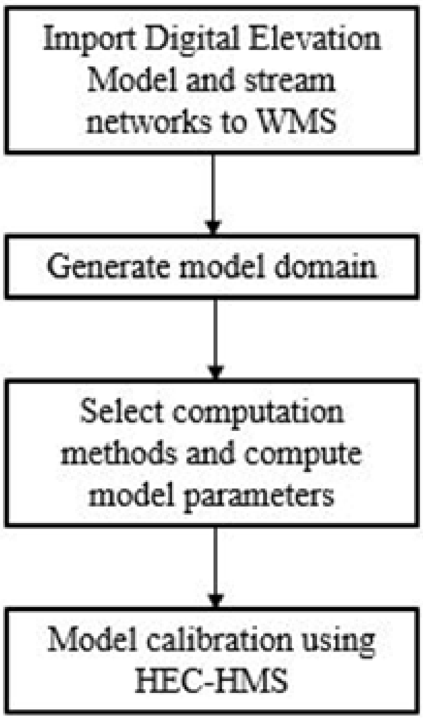

Figure 14. The Rainfall-Runoff Basin Model Development Scheme

Hydro-corrected SRTM DEM was used as the terrain for the basin model. The watershed delineation and its hydrologic elements, namely the subbasins, junctions and reaches, were generated using WMS after importing the elevation data and stream networks.

The parameters for the subbasins and reaches were computed after the model domain was created. There are several methods available for different calculation types for each subbasin and reach hydrologic elements. The methods used for this study is shown in Table 1. The necessary parameter values are determined by the selected methods. The initial abstraction, curve number, percentage impervious and manning's coefficient of roughness, n, for each subbasin were computed based on the soil type, land cover and land use data. The subbasin time of concentration and storage coefficient were computed based on the analysis of the topography of the basin.

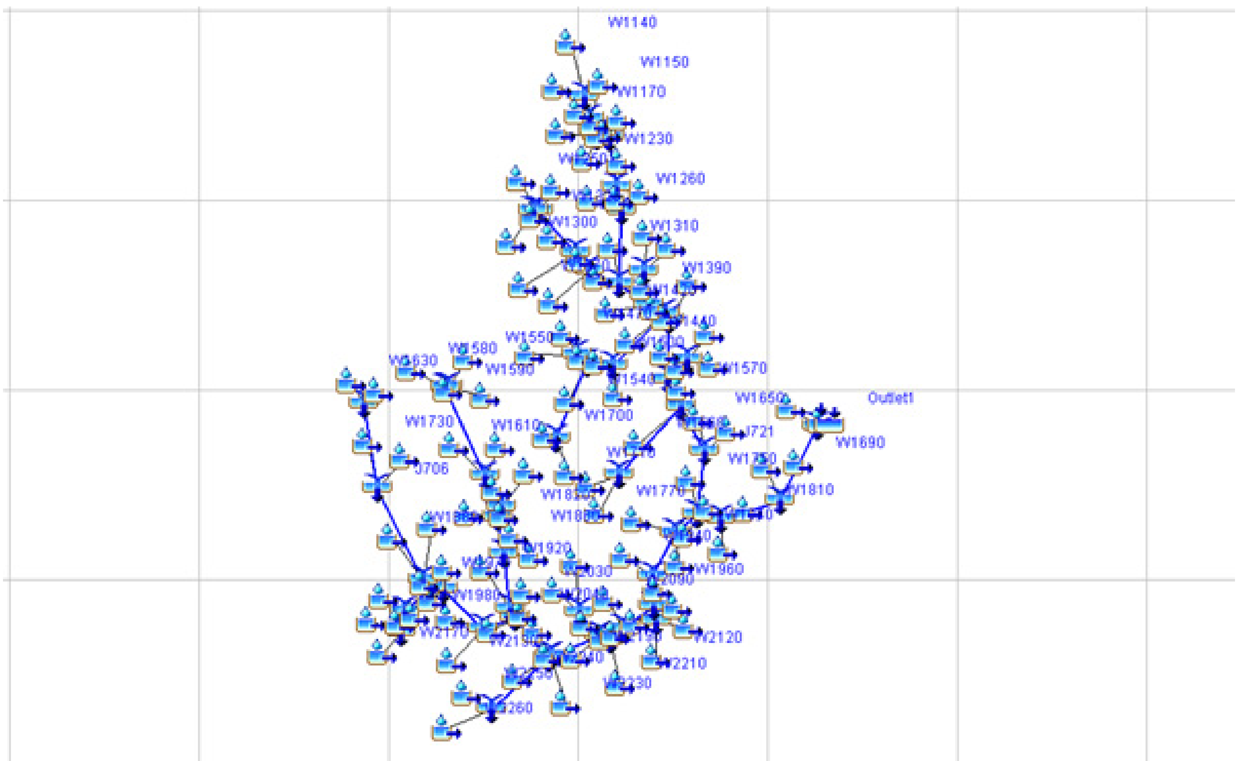

Figure 15. Infanta HEC-HMS Model domain generated by WMS

Table 1. Methods used for the different calculation types for the hydrologic elements

Hydrologic Element	Calculation Type	Method
Subbasin	Loss Rate	SCS Curve Number
	Transform	Clark's unit hydrograph
	Baseflow	Bounded recession
Reach	Routing	Muskingum-Cunge

3.2.2 Basin Model Calibration

The basin model made using WMS was exported to Hydrologic Modeling System (HEC-HMS) version 3.5, a software made by the Hydrologic Engineering Center of the US Army Corps of Engineers, to create the final rainfall-runoff model. The developers described HEC-HMS as a program designed to simulate the hydrologic processes of a dendritic watershed systems. In this study, the rainfall-runoff model was developed to calculate inflow from the watershed to the floodplain.

Precipitation data was taken from a sensor, an automatic rain gauge (ARGs) installed by the Department of Science and Technology – Advanced Science and Technology Institute (DOST-ASTI).

For the calibration of the downstream-most discharge point which is at Infanta Bridge, the total rain is 17.8 mm for one day. It peaked to 4.4 mm on 17 June 2013, 19:45.

The outflow hydrograph for the downstream-most discharge point with field data was also encoded to the model as a basis for the calibration. Using the said data, HEC-HMS could perform rainfall-runoff simulation and the resulting outflow hydrograph was compared with the observed hydrograph. The values of the parameters were adjusted and optimized in order for the calculated outflow hydrograph to appear like the observed hydrograph. Acceptable values of the subbasin and reach parameters from the manual and past literatures were considered in the calibration.

3.3 HEC-HMS Hydrologic Simulations for Discharge Computations using PAGASA RIDF Curves

3.3.1 Discharge Computation using Rainfall-Runoff Hydrologic Model

The calibrated rainfall-Runoff Hydrologic Model for the Infanta River Basin using WMS and HEC-HMS was used to simulate the flow for for the five return periods, namely, 5-, 10-, 25-, 50-, and 100-year RIDFs. Time-series data of the precipitation data using the Infanta RIDF curves were encoded to HEC-HMS for the aforementioned return periods, wherein each return period corresponds to a scenario. This process was performed for Infanta discharge point. The output for each simulation was an outflow hydrograph from that result, the total inflow to the floodplain and time difference between the peak outflow and peak precipitation could be determined.

3.3.2 Discharge Computation using Dr. Horritt's Recommended Hydrological Method

The required data to be accumulated for the implementation of Dr. Horrit's method is shown on Figure 16.

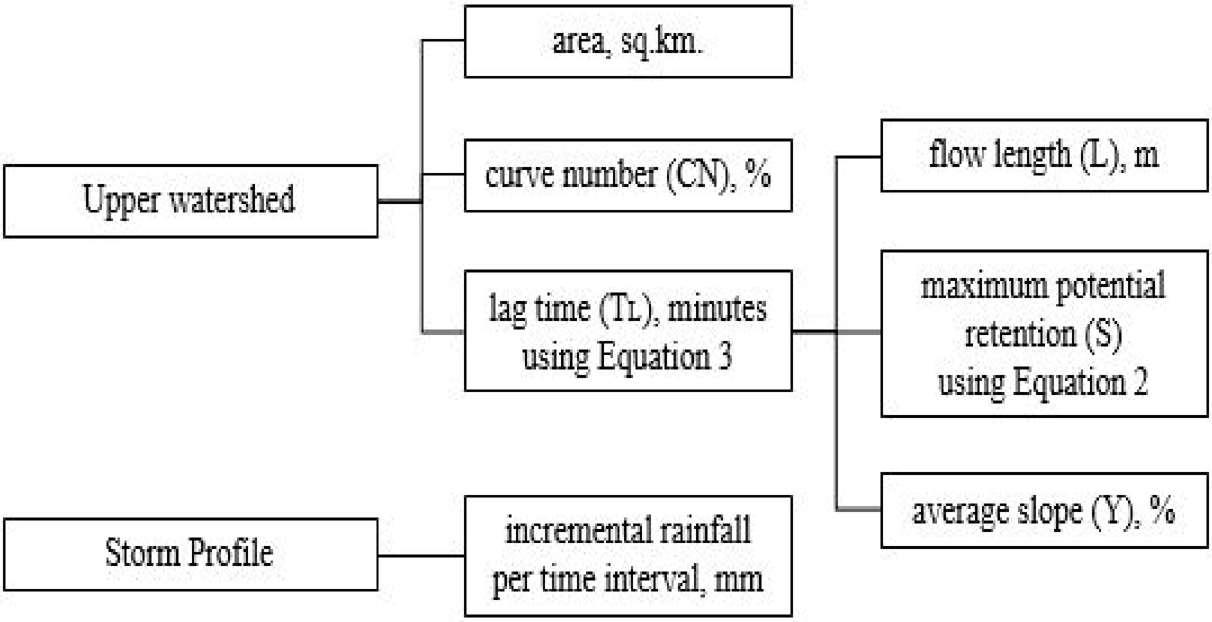

Figure 16. Different data needed as input for HEC-HMS discharge simulation using Dr. Horritt's recommended hydrology method

Flows from streams were computed using the hydrology method developed by the flood modeling component with Dr. Matt Horritt, a British hydrologist that specializes in flood research. The methodology was based on an approach developed by CH2M Hill and Horritt Consulting for Taiwan which has been successfully validated in a region with meteorology and hydrology similar to the Philippines. The method utilizes the SCS curve number and unit hydrograph method to have an accurate approximation of river discharge data from measurable catchment parameters.

3.3.2.1 Determination of Catchment Properties

RADARSAT DTM data for the different areas of the Philippines were compiled with the aid of ArcMap. RADARSAT satellites provide advance geospatial information and these were processed in the forms of shapefiles and layers that are readable and can be analyzed by ArcMap. These shapefiles are digital vectors that store geometric locations.

The watershed flow length is defined as the longest drainage path within the catchment, measured from the top of the watershed to the point of the outlet. With the tools provided by the ArcMap program and the data from RADARSAT DTM, the longest stream was selected and its geometric property, flow length, was then calculated in the program.

The area of the watershed is determined with the longest stream as the guide. The compiled RADARSAT data has a shapefile with defined small catchments based on mean elevation. These parameters were used in determining which catchments, along with the area, belong in the upper watershed.

Figure 17. Delineation of upper watershed for Infanta floodplain discharge computation

The value of the curve number was obtained using the RADARSAT data that contains information of the Philippine national curve number map. An ArcMap tool was used to determine the average curve number of the area bounded by the upper watershed shapefile. The same method was implemented in determining the average slope using RADARSAT with slope data for the whole country.

After determining the curve number (CN), the maximum potential retention (S) was determined by Equation 2.

$$S = \frac{1000}{CN} - 10$$

Equation 2. Determination of maximum potential retention using the average curve number of the catchment

The watershed length (L), average slope (Y) and maximum potential retention (S) are used to estimate the lag time of the upper watershed as illustrated in Equation 3.

$$T_L = \frac{L^{0.8}(S+1)^{0.7}}{560Y^{0.5}}$$

Equation 3. Lag Time Equation Calibrated for Philippine Setting

Finally, the final parameter that will be derived is the storm profile. The synoptic station which covers the majority of the upper watershed was identified. Using the RIDF data, the incremental values of rainfall in millimeter per 0.1 hour was used as the storm profile.

3.3.2.2 HEC-HMS Implementation

With all the parameters available, HEC-HMS was then utilized. Obtained values from the previous section were used as input and a brief simulation would result in the tabulation of discharge results per time interval. The maximum discharge and time-to-peak for the whole simulation as well as the river discharge hydrograph were used for the flood simulation process. The time series results (discharge per time interval) were stored as HYD files for input in FLO-2D GDS Pro.

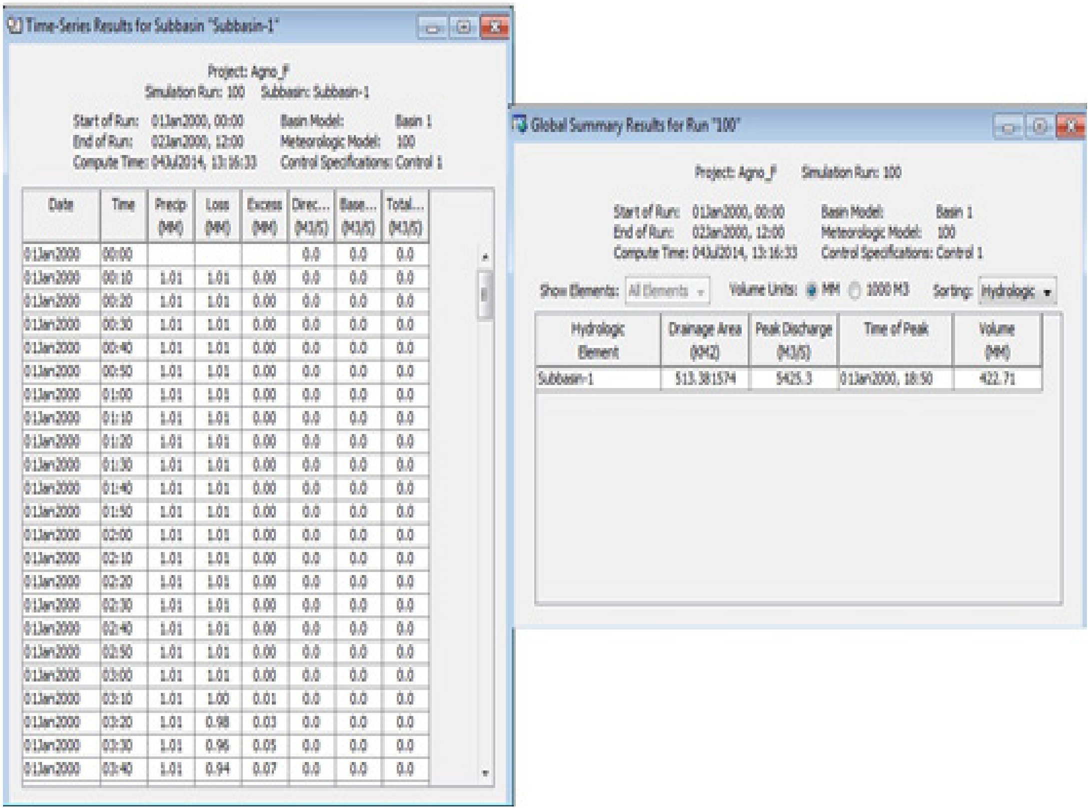

Figure 18. HEC-HMS simulation discharge results using Dr. Horritt's Method

3.3.2.3 Discharge validation against other estimates

As a general rule, the river discharge of a 2-year rain return, Q_{MED}, should approximately be equal to the bankful discharge, $Q_{bankful}$, of the river. This assumes that the river is in equilibrium, with its deposition being balanced by erosion. Since the simulations of the river discharge are done for 5-, 25-, and 100-year rainfall return scenarios, a simple ratio for the 2-year and 5-year return was computed with samples from actual discharge data of different rivers. It was found out to have a constant of 0.88. This constant, however, should still be continuously checked and calibrated when necessary.

$$Q_{MED} = 0.88Q_{5yr}$$

Equation 4. Ratio of river discharge of a 5-year rain return to a 2-year rain return scenario from measured discharge data

For the discharge calculation to pass the validation using the bankful method, Equation 5 must be satisfied.

$$50\%\, Q_{bankful} \leq Q_{MED} \leq 150\%\, Q_{bankful}$$

Equation 5. Discharge validation equation using bankful method

The bankful discharge was estimated using channel width (w), channel depth (h), bed slope (S) and Manning's constant (n). Derived from the Manning's Equation, the equation for the bankful discharge is by Equation 6.

$$Q_{bankful} = \frac{(wh)^{\frac{5}{3}} S^{\frac{1}{2}}}{n(w+2h)^{\frac{2}{3}}}$$

Equation 6. Bankful discharge equation using measurable channel parameters

3.4 Hazard and Flow Depth Mapping using FLO-2D

3.4.1 Floodplain Delineation

The boundaries of subbasins within the floodplain were delineated based on elevation values given by the DEM. Each subbasin is marked by ridges dividing catchment areas. These catchments were delineated using a set of ArcMap tools compiled by Al Duncan, a UK Geomatics Specialist, into a single processing model. The tool allows ArcMap to compute for the flow direction and acceleration based on the elevations provided by the DEM.

Running the tool creates features representing large, medium-sized, and small streams, as well as large, medium-sized, and small catchments. For the purpose of this particular model, the large, medium-sized, and small streams were set to have an area threshold of 100,000sqm, 50,000sqm, and 10,000sqm respectively. These thresholds define the values where the algorithm refers to in delineating a trough in the DEM as a stream feature, i.e. a large stream feature should drain a catchment area totalling 100,000 sqm to be considered as such. These values differ from the standard values used (10,000sqm, 1,000 sqm and 100sqm) to limit the detail of the project, as well as the file sizes, allowing the software to process the data faster.

The tool also shows the direction in which the water is going to flow across the catchment area. This information was used as the basis for delineating the floodplain. The entire area of the floodplain was subdivided into several zones in such a way that it can be processed properly. This was done by grouping the catchments together, taking special account of the inflows and outflows of water across the entire area. To be able to simulate actual conditions, all the catchments comprising a particular computational domain were set to have outflows that merged towards a single point. The area of each subdivision was limited to 250,000 grids or less to allow for an optimal simulation in FLO-2D GDS Pro. Larger models tend to run longer, while smaller models may not be as accurate as a large one.

3.4.2 Flood Model Generation

The software used to run the simulation is FLO-2D GDS Pro. It is a GIS integrated software tool that creates an integrated river and floodplain model by simulating the flow of the water over a system of square grid elements.

After loading the shapefile of the subcatchment onto FLO-2D, 10 meter by 10 meter grids that encompassed the entire area of interest were created.

The boundary for the area was set by defining the boundary grid elements. This can either be done by defining each element individually, or by drawing a line that traces the boundaries of the subcatchment. The grid elements inside of the defined boundary were considered as the computational area in which the simulation will be run.

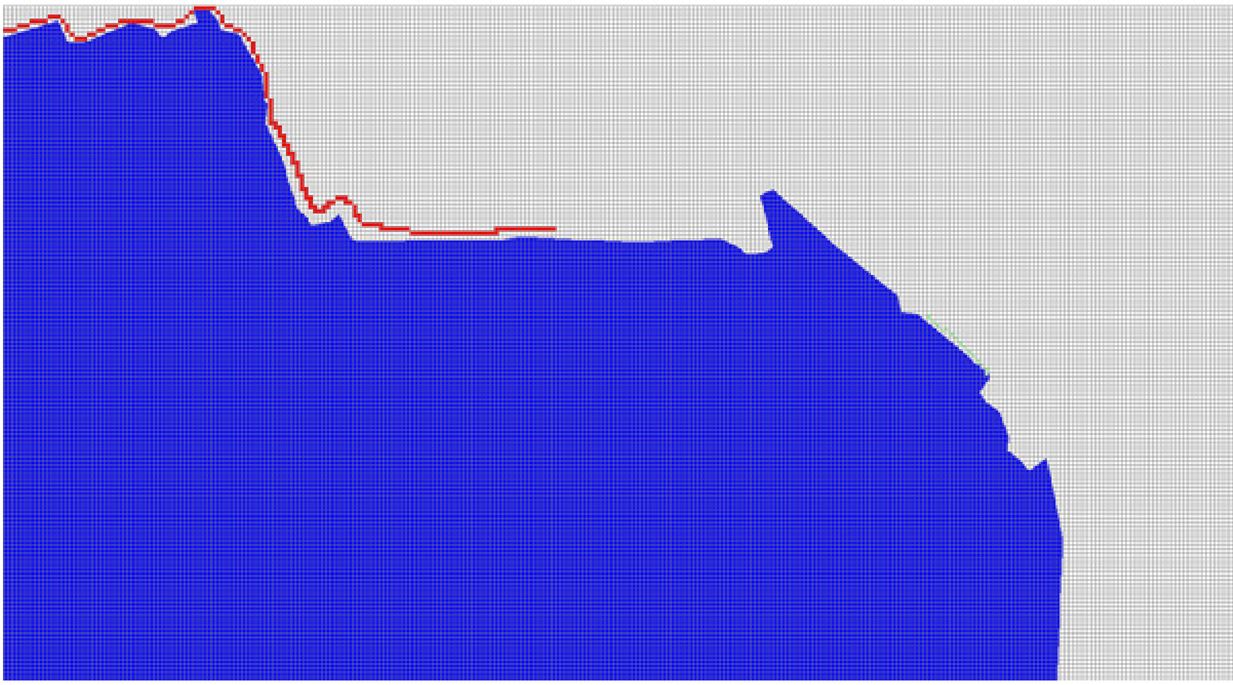

Figure 19. Screenshot showing how boundary grid elements are defined by line

Elevation data was imported in the form of the DEM gathered through LiDAR. These elevation points in PTS format were extrapolated into the model, providing an elevation value for each grid element.

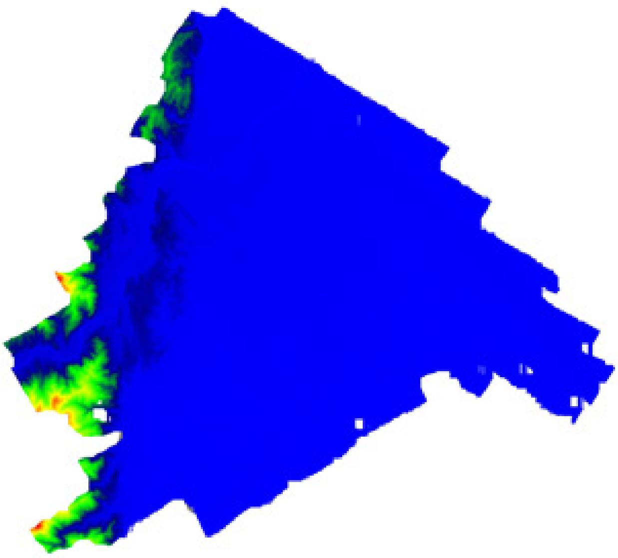

Figure 20. Screenshots of PTS files when loaded into the FLO-2D program

The floodplain is predominantly composed of rice fields, which have a Manning coefficient of 0.15. All the inner grid elements were selected and the Manning coefficient of 0.15 was assigned. To differentiate the streams from the rest of the floodplain, a shapefile containing all the streams and rivers in the area were imported into the software. The shapefile was generated using Al Duncan's catchment tool for ArcMap. The streams were then traced onto their corresponding grid elements.

These grid elements were all selected and assigned a Manning coefficient of 0.03. The DEM and aerial imagery were also used as bases for tracing the streams and rivers.

Figure 21. Areal image of Infanta floodplain

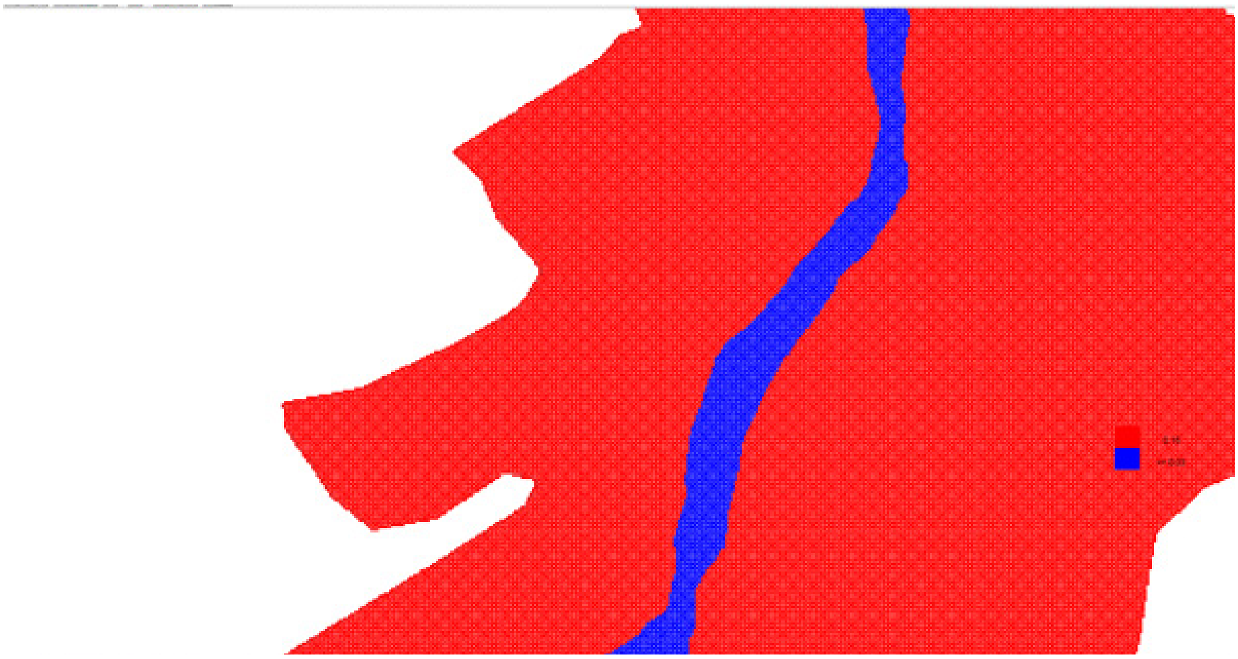

Figure 22. Screenshot of Manning's n-value rendering

After assigning Manning coefficients for each grid, the infiltration parameters were identified. Green-Ampt infiltration method by W. Heber Green and G.S Ampt were used for all the models. The initial saturations applied to the model were 0.99, 0.8, and 0.7 for 100-year, 25-year, and 5-year rain return periods respectively. These initial saturations were used in the computation of the infiltration value.

The Green-Ampt infiltration method by W. Heber Green and G.S Ampt method is based on a simple physical model in which the equation parameter can be related to physical properties of the soil. Physically, Green and Ampt assumed that the soil was saturated behind the wetting front and that one could define some "effective" matric potential at the wetting front (Kirkham, 2005). Basically, the system is assumed to consist of a uniformly wetted near-saturated transmission zone above a sharply defined wetting front of constant pressure head (Diamond & Shanley, 2003).

The next step was to allocate inflow nodes based on the locations of the outlets of the streams from the upper watershed. The inflow values came from the computed discharges that were input as hyd files.

Outflow nodes were allocated for the model. These outflow nodes show the locations where the water received by the watershed is discharged. The water that will remain in the watershed will result to flooding on low lying areas.

For the models to be able to simulate actual conditions, the inflow and outflow of each computational domain should be indicated properly. In situations wherein water flows from one subcatchment to the other, the corresponding models are processed one after the other. The outflow generated by the source subcatchment was used as inflow for the subcatchment area that it flows into.

The standard simulation time used to run each model is the time-to-peak (TP) plus an additional 12 hours. This gives enough time for the water to flow into and out of the model area, illustrating the complete process from entry to exit as shown in the hydrograph. The additional 12 hours allows enough time for the water to drain fully into the next subcatchment. After all the parameters were set, the model was run through FLO-2D GDS Pro.

3.4.3 Flow Depth and Hazard Map Simulation

After running the flood map simulation in FLO-2D GDS Pro, FLO-2D Mapper Pro was used to read the resulting hazard and flow depth maps. The standard input values for reading the simulation results are shown on Figure 24.

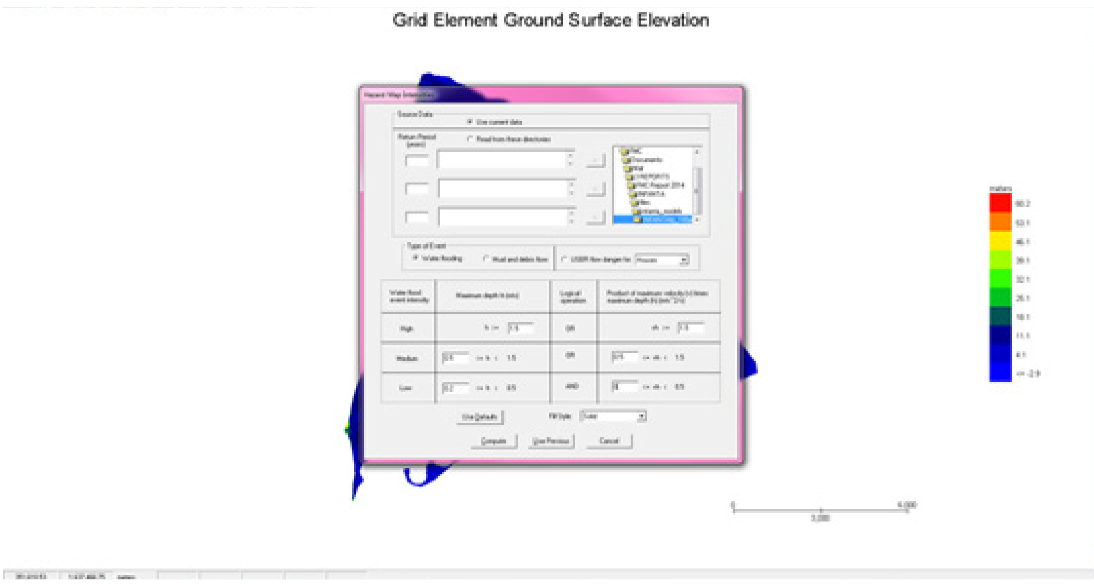

Figure 23. Flo-2D Mapper Pro General Procedure

In order to produce the hazard maps, set input for low maximum depth as 0.2 m, and vh, product of maximum velocity and maximum depth (m^2/s), as greater than or equal to zero. The program will then compute for the flood inundation and will generate shapefiles for the hazard and flow depth scenario.

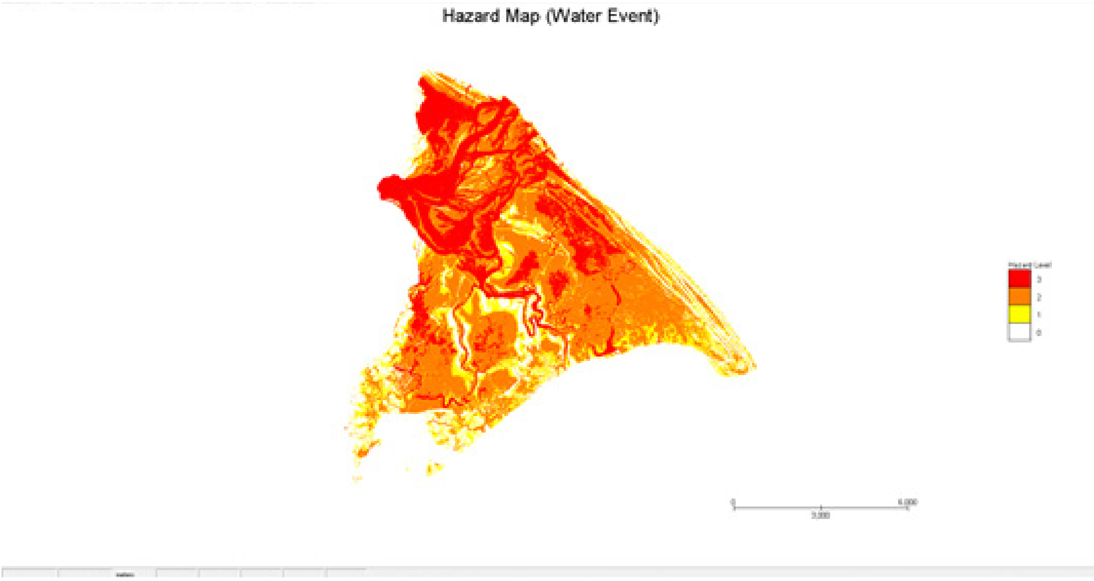

Figure 24. Infanta Floodplain Generated Hazard Maps using FLO-2D Mapper

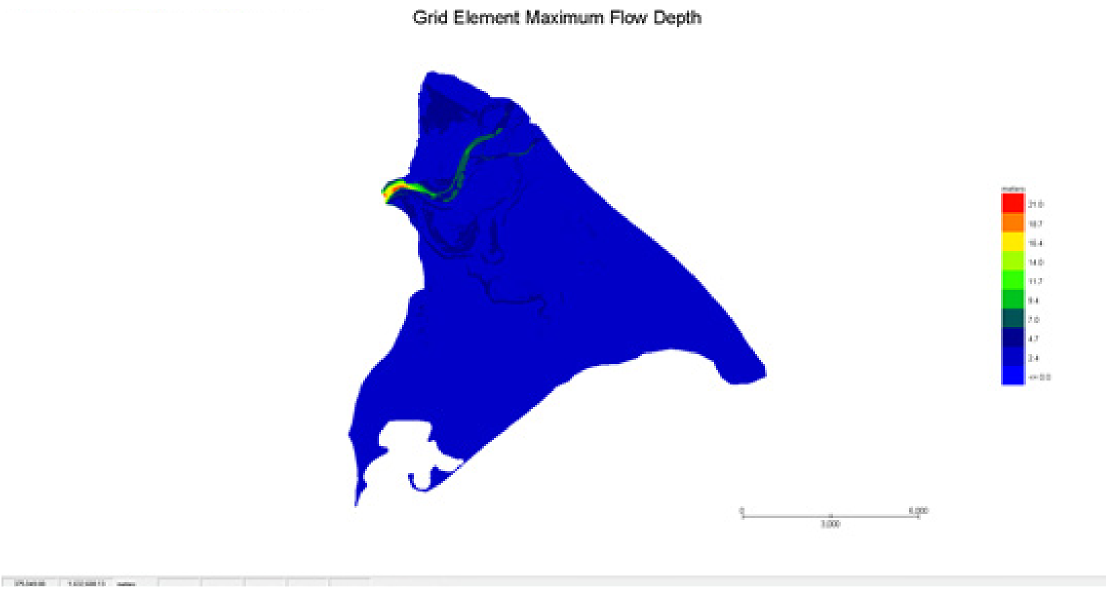

Figure 25. Infanta floodplain generated flow depth map using FLO-2D Mapper

3.4.4 Hazard Map and Flow Depth Map Creation

The final procedure in creating the maps is to prepare them with the aid of ArcMap. The generated shapefiles from FLO-2D Mapper Pro were opened in ArcMap. The basic layout of a hazard map is shown in Figure 27. The same map elements are also found in a flow depth map.

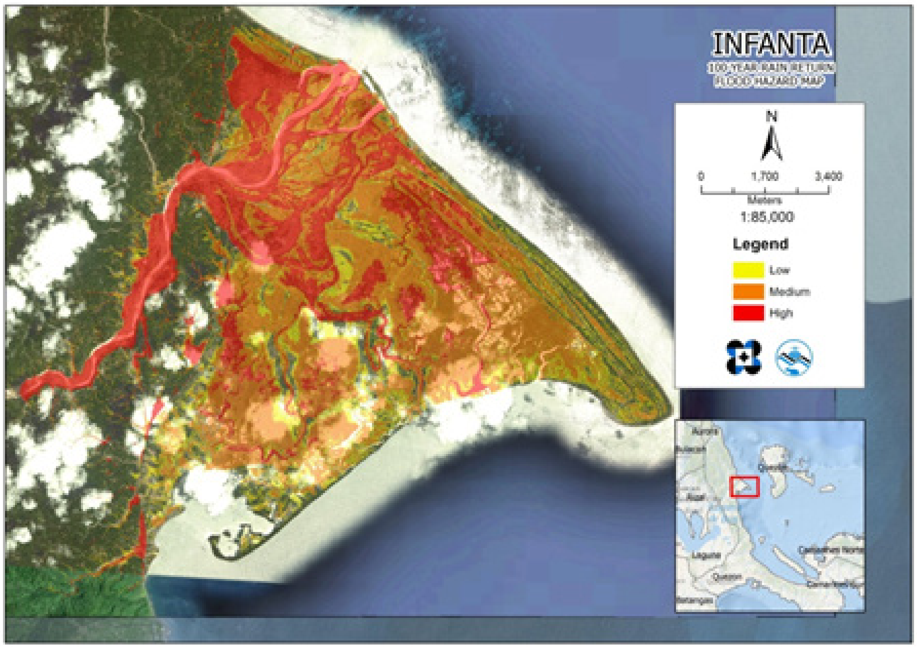

ELEMENTS
1. River Basin Name
2. Hazard/Flow Depth Shapefile
3. Provincial Inset
4. Philippine Inset
5. Hi-Res image of the area
6. North Arrow
7. Scale text and Bar

Figure 26. Basic Layout and Elements of the Hazard Maps

Results and Discussion

4.1 Efficiency of HEC-HMS Rainfall-Runoff Models calibrated based on field survey and gauges data

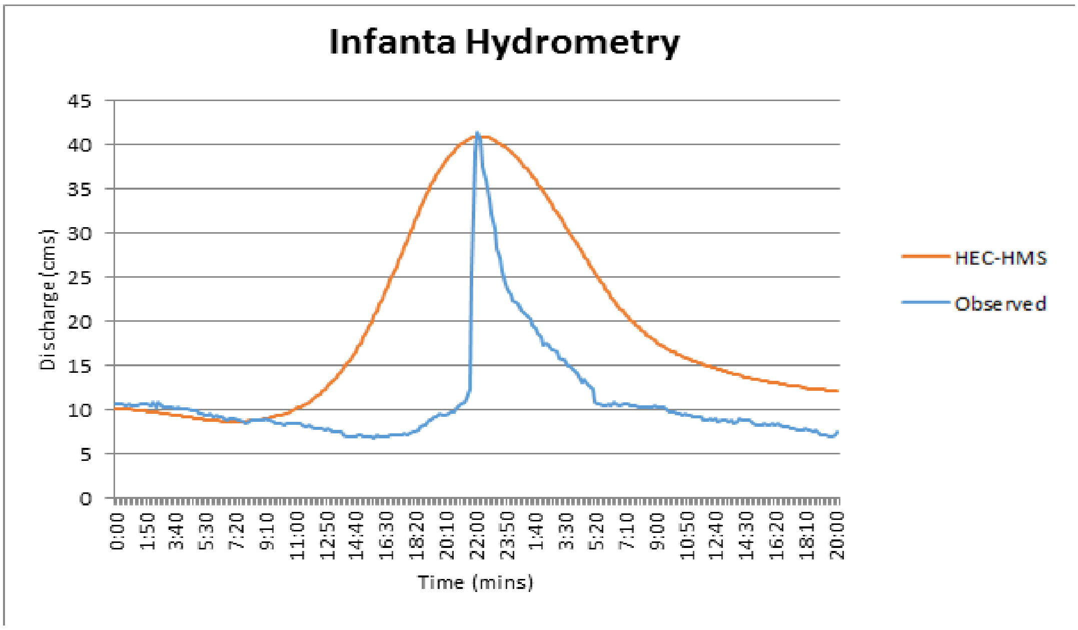

Figure 27. Infanta Outflow Hydrograph produced by the HEC-HMS model compared with observed outflow

After calibrating the Infanta HEC-HMS river basin model, its accuracy was measured against the observed values. Figure 37 shows the comparison between the two discharge data.

The Root Mean Square Error (RMSE) method aggregates the individual differences of these two measurements. It was identified at 11.8.

The Pearson correlation coefficient (r2) assesses the strength of the linear relationship between the observations and the model. This value being close to 1 corresponds to an almost perfect match of the observed discharge and the resulting discharge from the HEC HMS model. Here, it measured 0.6420.

The Nash-Sutcliffe (E) method was also used to assess the predictive power of the model. Here the optimal value is 1. The model attained an efficiency coefficient of -2.92.

A positive Percent Bias (PBIAS) indicates a model's propensity towards under-prediction. Negative values indicate bias towards over-prediction. Again, the optimal value is 0. In the model, the PBIAS is -43.23.

The Observation Standard Deviation Ratio, RSR, is an error index. A perfect model attains a value of 0 when the error in the units of the valuable a quantified. The model has an RSR value of 1.98.

The calibrated models of the other discharge points are used in flood forecasting. DREAM Program offers the LGUs and other disaster mitigation agencies a water level forecast tool, which can be found on the DREAM website.

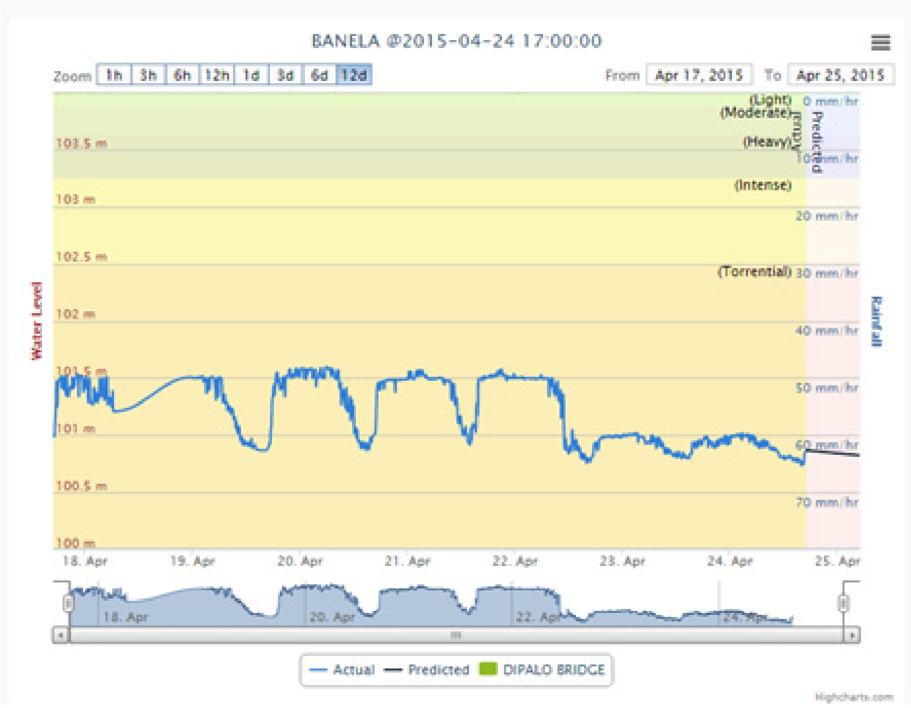

Figure 28. Sample DREAM Water Level Forecast

Given the predicted and real-time actual water level on specific AWLS, possible river flooding can be monitored and information can be disseminated to LGUs. This will help in the early evacuation of the probable affected communities. The calibrated models can also be used for flood inundation mapping.

4.2 Calculated Outflow hydrographs and Discharge Values for different Rainfall Return Periods

4.2.1 Hydrograph using the Rainfall-Runoff Model

The outflow of Infanta using the Infanta station Rainfall Intensity-Duration-Frequency curves (RIDF) in 5 different return periods (5-year, 10-year, 25-year, 50-year, and 100-year rainfall time series) based on PAGASA data are shown in Figures 30-34. The simulation results reveal significant increase in outflow magnitude as the rainfall intensity increases for a range of durations and return periods.

In the 5-year return period graph, the peak outflow is 2731.7 cms. This occurs after 9 hours after the peak precipitation of 25.7 mm, as shown on Figure 30.

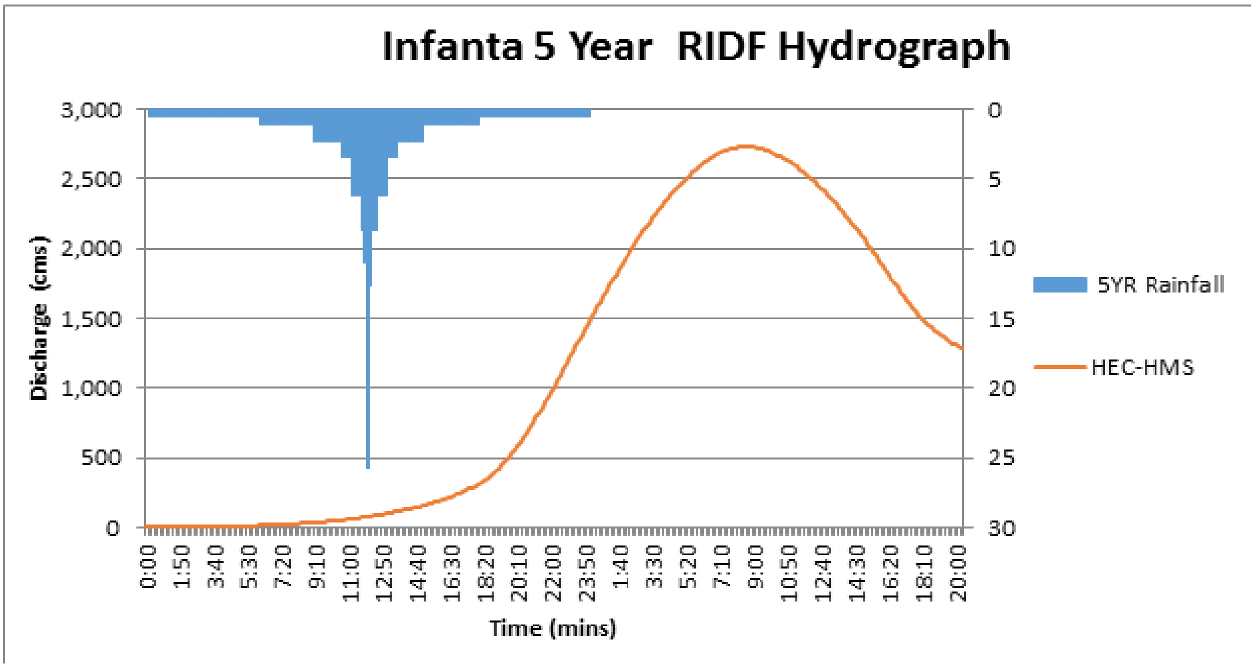

Figure 29. Infanta outflow hydrograph generated using the Infanta 5-Year RIDF in HEC-HMS

In the 10-year return period graph, the peak outflow is 2873.6 cms. This occurs after 8 hours after the peak precipitation of 29.2 mm, as shown on Figure 31.

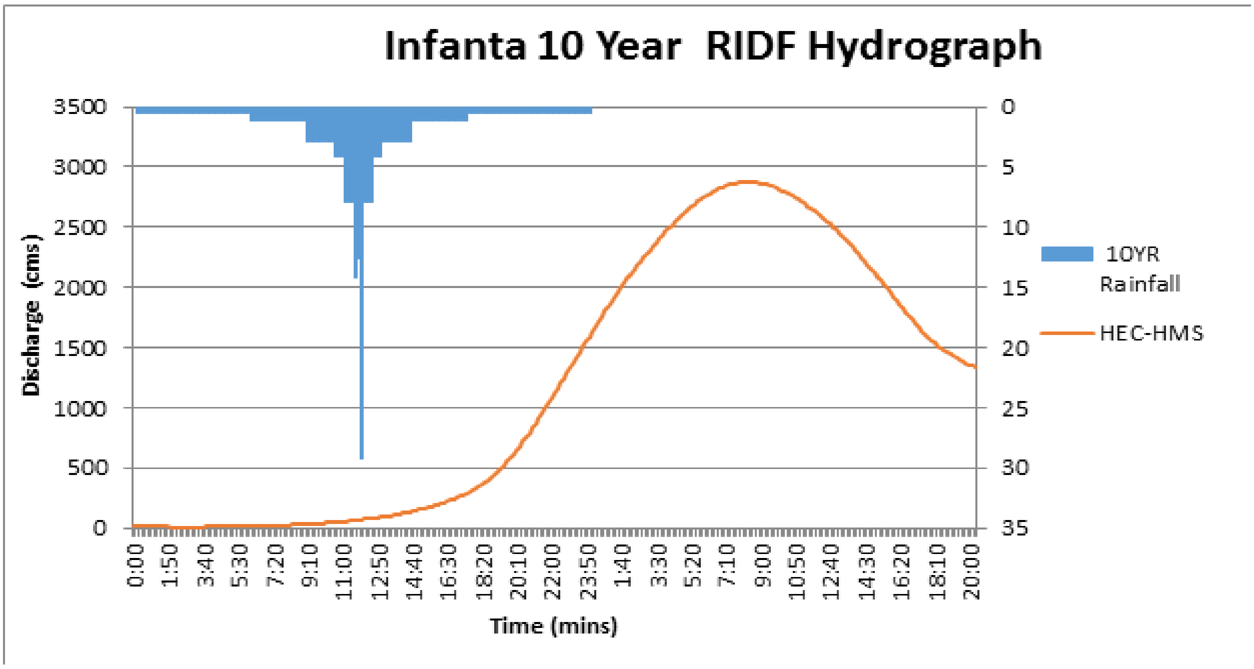

Figure 30. Infanta outflow hydrograph generated using the Infanta 10-Year RIDF in HEC-HMS

In the 25-year return period graph, the peak outflow is 165.5 cms. This occurs after 15 hours and 10 minutes, and a precipitation of 30.79 mm, as shown on Figure 32.

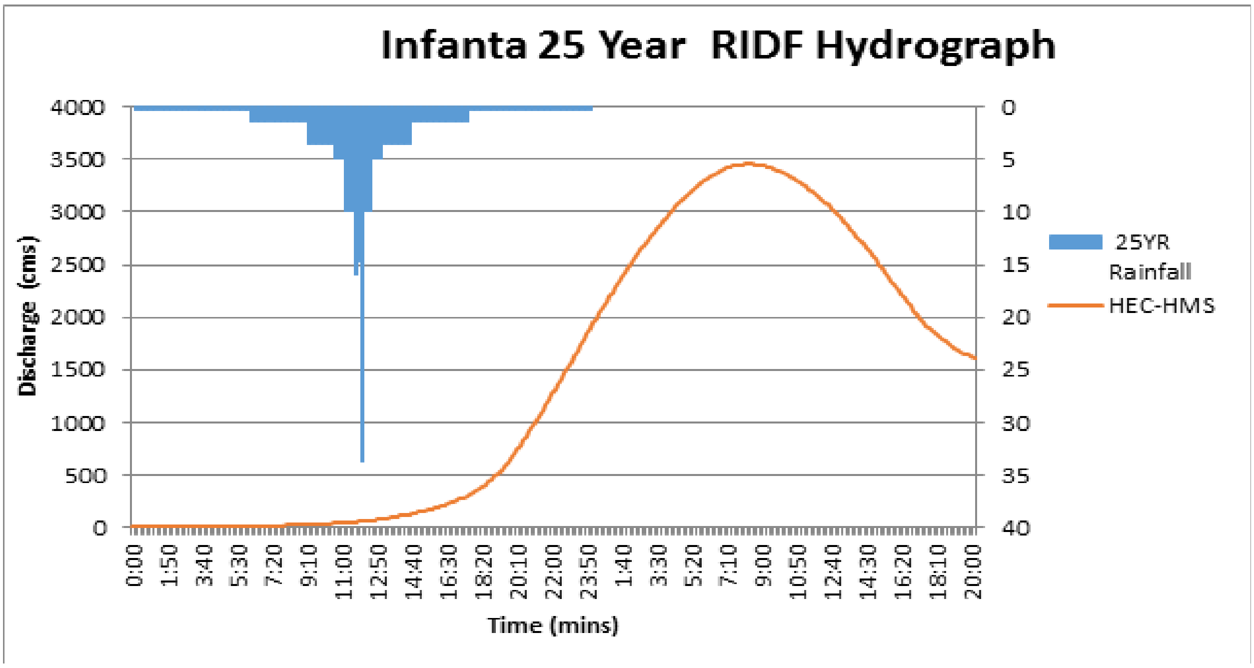

Figure 31. Infanta Outflow hydrograph generated using the Infanta 25-Year RIDF in HEC-HMS

In the 50-year return period graph, the peak outflow is 3887.6 cms. This occurs after 6 hours and 40 minutes after the peak precipitation of 37 mm, as shown on Figure 33.

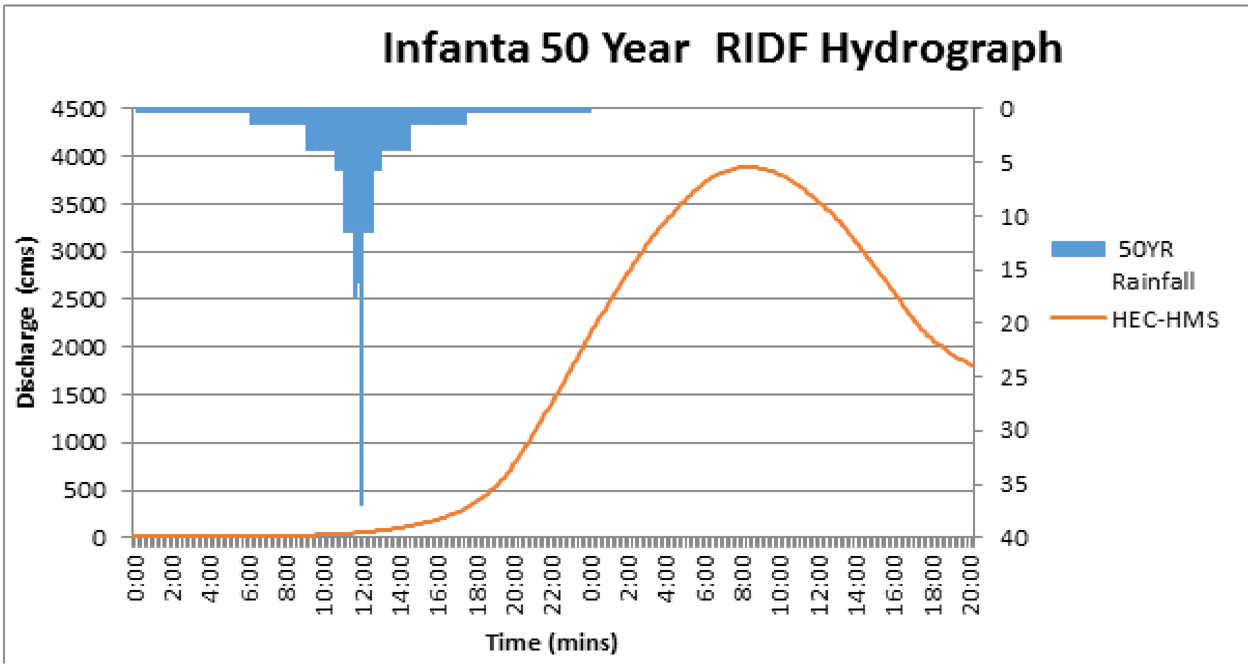

Figure 32. Infanta outflow hydrograph generated using the Infanta 50-Year RIDF in HEC-HMS

In the 100-year return period graph, the peak outflow is 4315.4 cms. This occurs after 7 hours and 40 minutes after the peak precipitation of 40.3 mm, as shown on Figure 34.

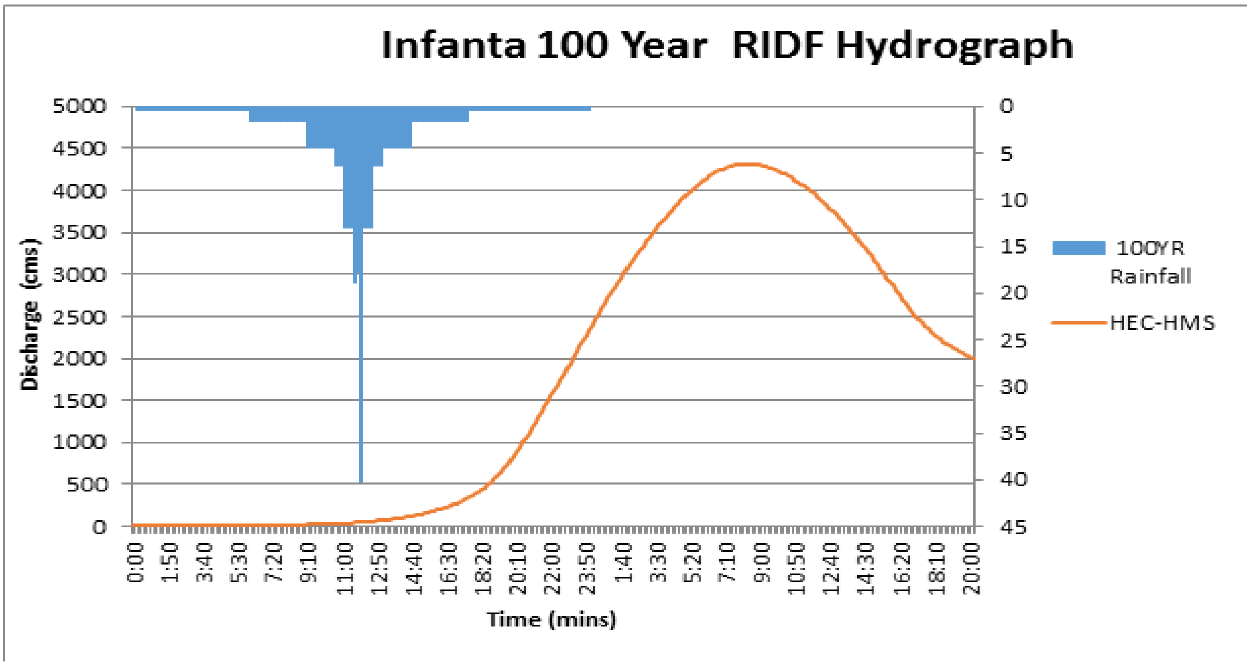

Figure 33. Infanta Outflow hydrograph generated using the Infanta 100-Year RIDF in HEC-HMS

A summary of the total precipitation, peak rainfall, peak outflow and time to peak of Infanta discharge using the Infanta Rainfall Intensity-Duration-Frequency curves (RIDF) in five different return periods is shown in Table 2.

Table 2. Summary of Infanta discharge using Infanta Station Rainfall Intensity Duration Frequency (RIDF)

RIDF Period	Total Precipitation (mm)	Peak rainfall (mm)	Peak outflow (cms)	Time to Peak
5-Year	249.6	25.7	2731.7	9 hours
10-Year	287.1	29.2	2873.6	8 hours
25-Year	334.4	33.7	3453.7	8 hours and 30 minutes
50-Year	369.6	37	3887.6	6 hours and 40 minutes
100-Year	404.4	40.3	4315.4	7 hours and 40 minutes

4.2.2 Discharge Data using Dr. Horritt's Recommended Hydrological Method

The river discharge values using Dr. Horritt's recommended hydrological method are shown in Figure 35 and the peak discharge values are summarized in Table 3.

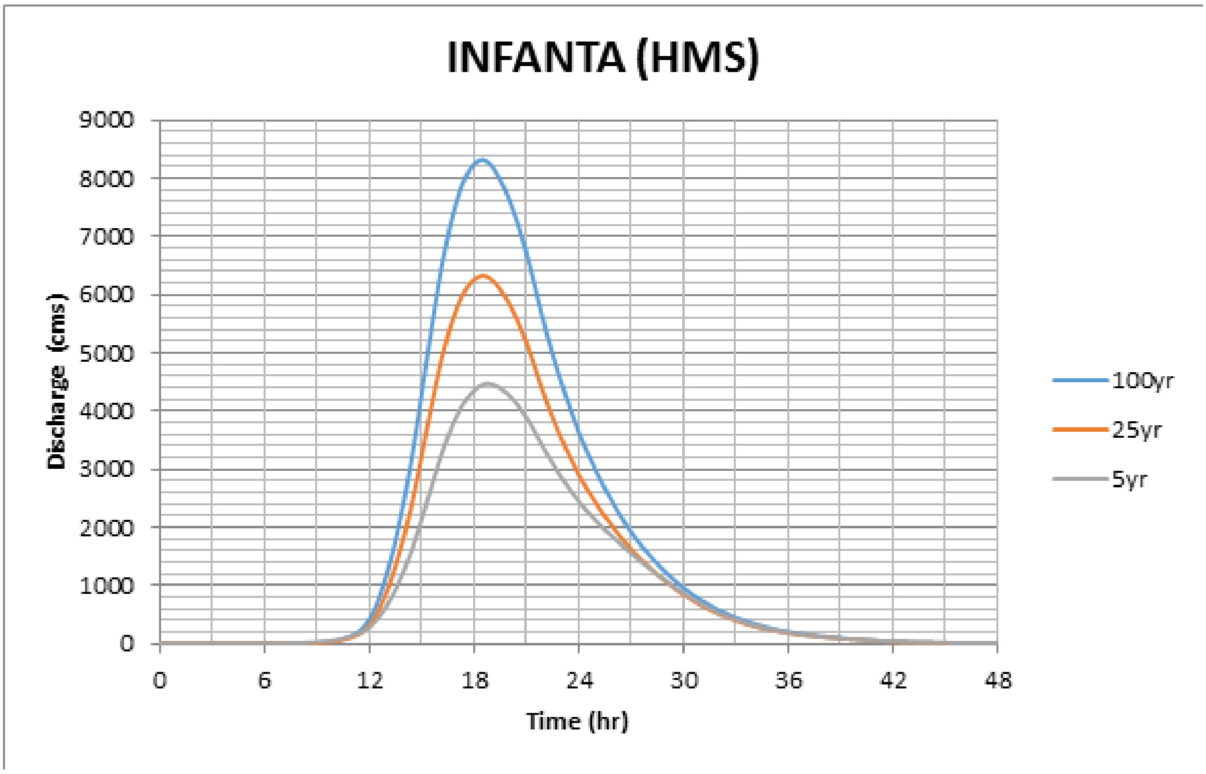

Figure 34. Outflow hydrograph generated using the Infanta 5-,25-, 100-Year RIDF in HEC-HMS.

Table 3. Summary of Infanta river discharge using the recommended hydrological method by Dr. Horritt

RIDF Period	Peak discharge (cms)	Time-to-peak
5-Year	4464.3	18 hours, 50 minutes
25-Year	6326.9	18 hours, 30 minutes
100-Year	8317.7	18 hours, 30 minutes

The comparison of discharge values obtained from HEC-HMS, Q5yr, and from the bankful discharge method, Qbankful, are shown in Table 4. Using values from the DTM of Infanta, the bankful discharge for the river was computed.

Table 4. Validation of river discharge estimate

Floodplain	Qbankful, cms	Q5yr, cms	Validation
Infanta (1)	6126.24	3928.58	Pass

The value from the HEC-HMS discharge estimate was able to satisfy the conditions for validating the computed discharge using the bankful method. Since the computed values are based on theory, the actual discharge values were still used for flood modeling but will need further investigation for the purpose of validation. It is recommended, therefore, to use the actual value of the river discharge for higher-accuracy modeling.

4.3 Flood Hazard and Flow Depth Maps

The following images are the hazard and flow depth maps for the 5-, 25-, and 100-year rain return scenarios of the Infanta river basin.

Results and Discussion

Flood Hazard Maps and Flow Depth Maps

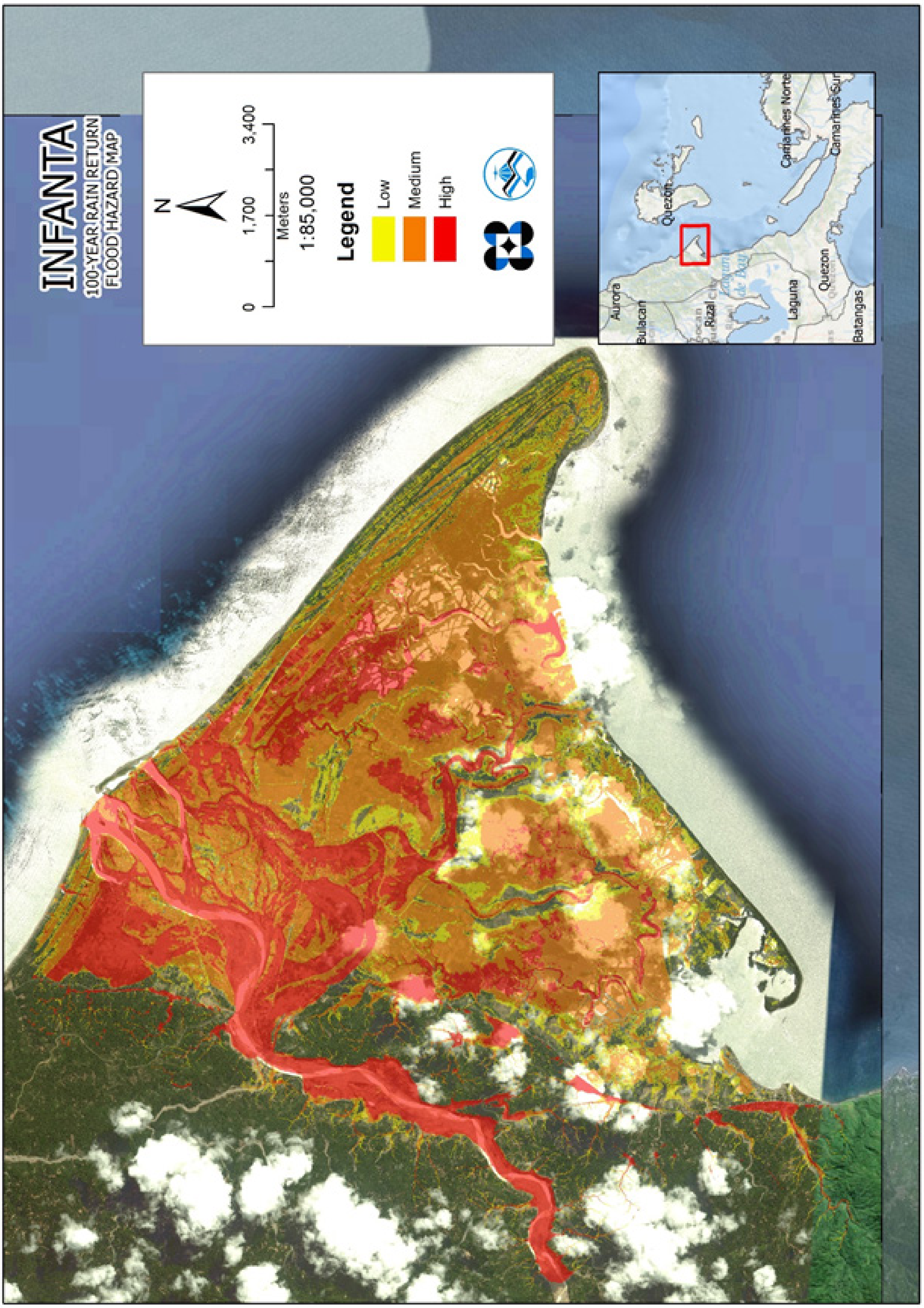

Figure 35. 100-year Flood Hazard Map for Infanta River Basin

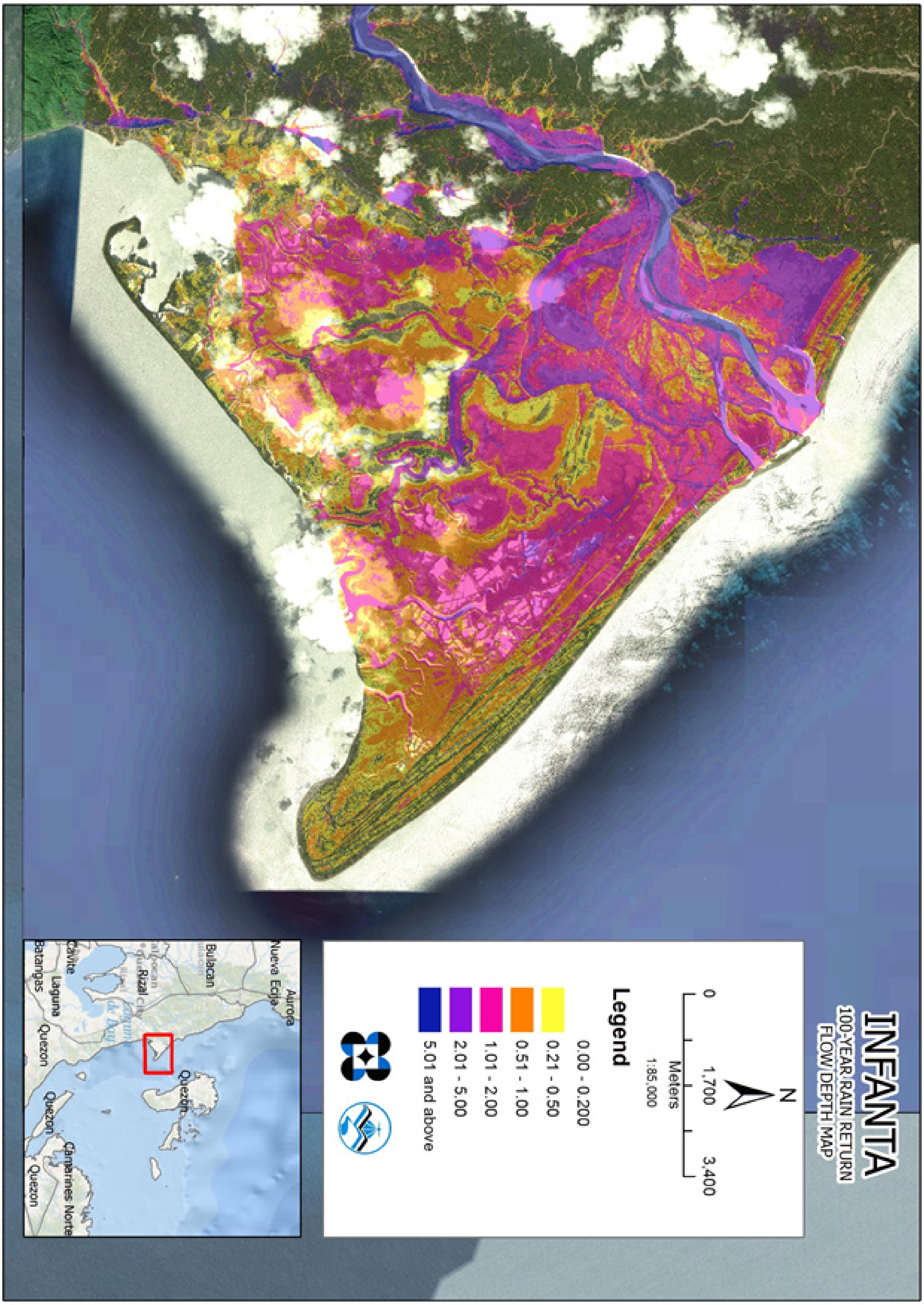

Figure 36. 100-year Flow Depth Map for Infanta River Basin

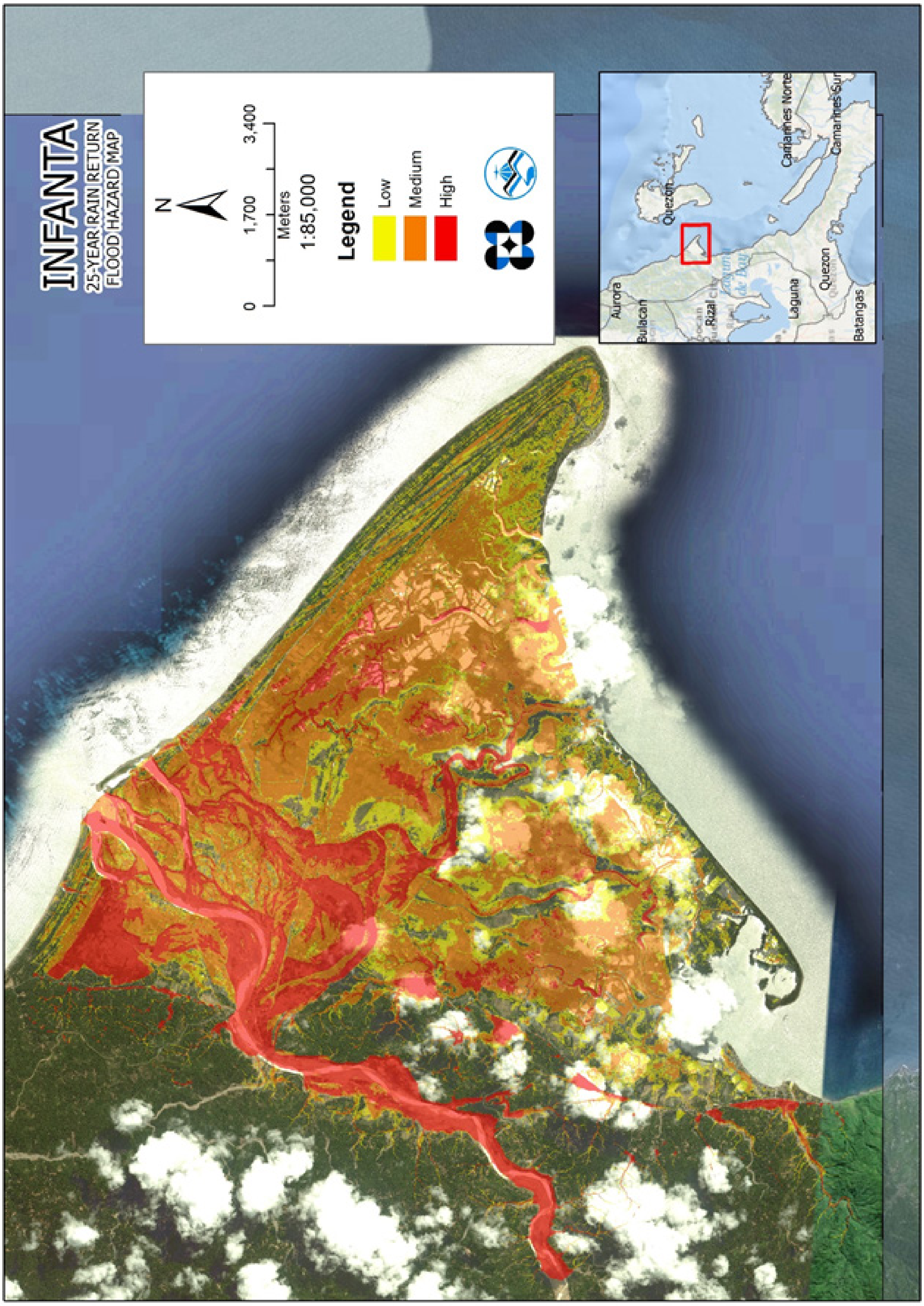

Figure 37. 25-year Flood Hazard Map for Infanta River Basin

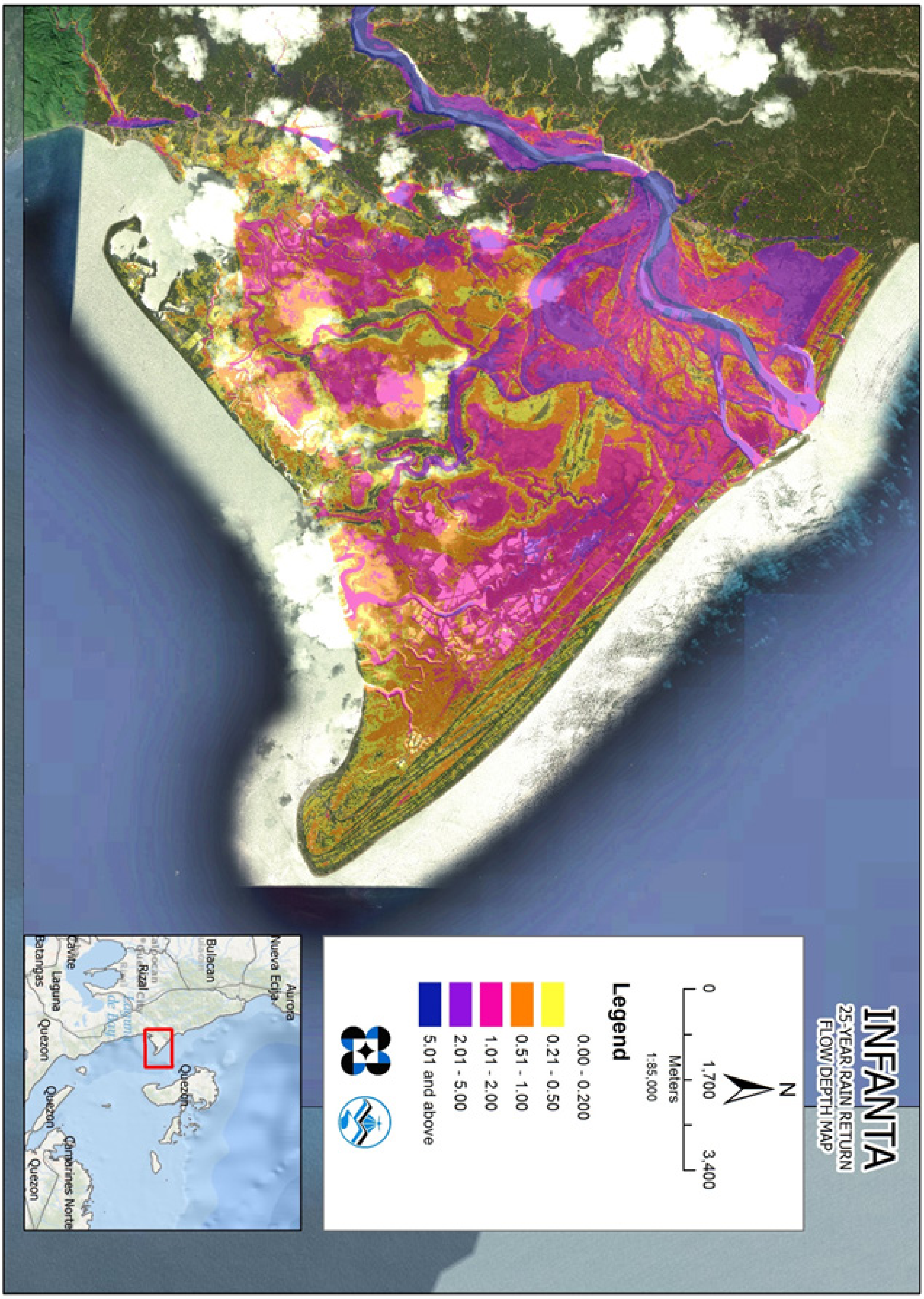

Figure 38. 25-year Flow Depth Map for Infanta River Basin

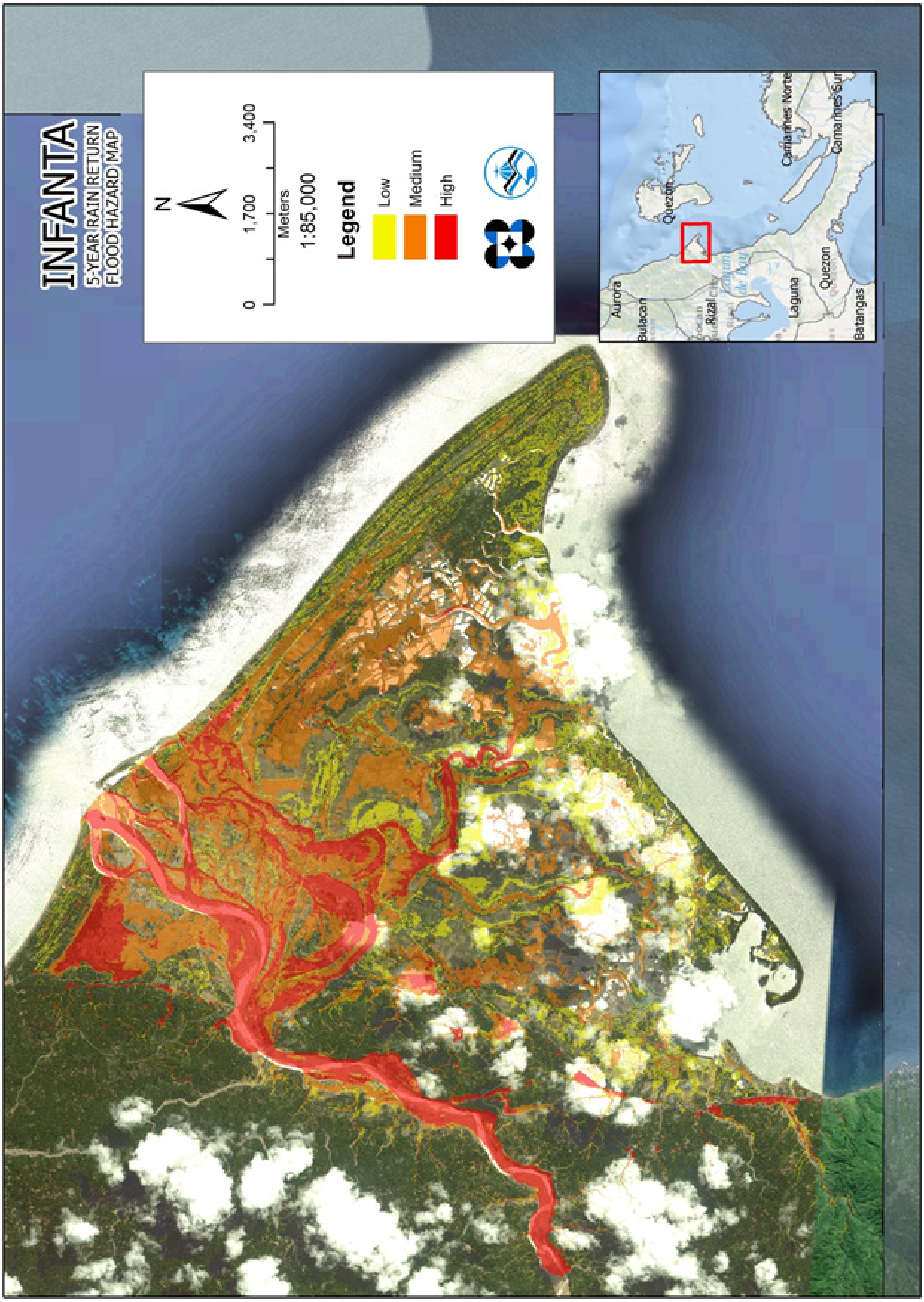

Figure 39. 5-year Flood Hazard Map for Infanta River Basin

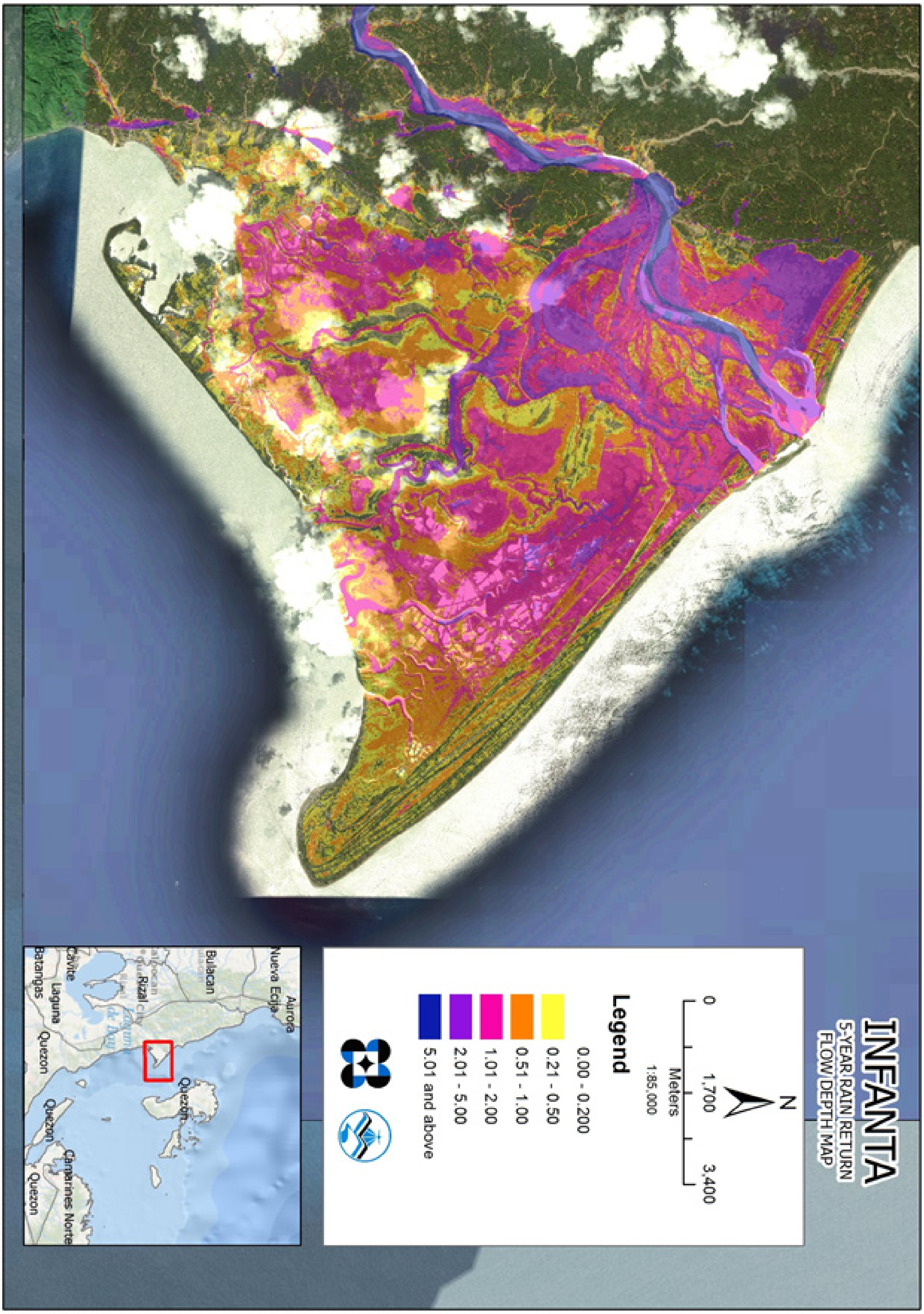

Figure 40. 5-year Flood Hazard Map for Infanta River Basin

Bibliography

- Aquaveo. (2012). Watershed Modeling - HEC HMS Interface. Aquaveo.
- Feldman, A. D. (2000). Hydrologic Modeling System HEC-HMS Technical Reference Manual. Davis, CA: US Army Corps of Engineers - Hydrologic Engineering Center.
- FLO-2D Software, I. Flo-2D Reference Manual. FLO-2D Software, Inc.
- Merwade, V. (2012). Terrain Processing and HMS- Model Development using GeoHMS. Lafayette, Indiana.
- Santillan, J. (2011). Profile and Cross Section Surveys, Inflow measurement and flood modeling of Surigao River, Surigao City for Flood Hazard Assessment Purposes. Quezon City: Training Center for Applied Geodesy and Photogrammetry (TCAGP).
- Scharffenberg, W. A., & Fleming, M. J. (2010). Hydrologic Modeling System HEC-HMS User's Manual. Davis, California: U.S Army Corps of Engineers - Hydrologic Engineering Center.

Appendix

Appendix A. Infanta Model Basin Parameters

Basin Number	SCS Curve Number Loss			Clark Unit Hydrograph Transform		Recession Baseflow				
	Initial Abstraction (mm)	Curve Number	Impervious (%)	Time of Concentration (HR)	Storage Coefficient (HR)	Initial Type	Initial Discharge (M3/S)	Recession Constant	Threshold Type	Ratio to Peak
W1140	0.207666	94.5	0	22.9	4.340236	Discharge	0.15289	1	Ratio to Peak	0.5
W1150	0.180482	94.5	0	22.9	3.344087	Discharge	0.0966392	1	Ratio to Peak	0.5
W1160	0.207	94.5	0	22.9	2.720615	Discharge	0.0699925	1	Ratio to Peak	0.5
W1170	0.207	94.5	0	22.9	1.350166	Discharge	0.0156382	1	Ratio to Peak	0.5
W1180	0.187834	94.5	0	22.9	1.493513	Discharge	0.0216605	1	Ratio to Peak	0.5
W1190	0.151171	94.5	0	22.9	0.72175	Discharge	0.0021581	1	Ratio to Peak	0.5
W1200	0.19759	94.5	0	22.9	0.646761	Discharge	0.0040639	1	Ratio to Peak	0.5
W1210	0.207	94.5	0	22.9	2.134631	Discharge	0.0570621	1	Ratio to Peak	0.5
W1220	0.206861	94.5	0	22.9	2.92547	Discharge	0.0990314	1	Ratio to Peak	0.5
W1230	0.205693	94.5	0	22.9	1.999151	Discharge	0.0567078	1	Ratio to Peak	0.5
W1240	0.207	94.5	0	22.9	2.501333	Discharge	0.0891191	1	Ratio to Peak	0.5

Basin Number	SCS Curve Number Loss			Clark Unit Hydrograph Transform		Recession Baseflow				
	Initial Abstraction (mm)	Curve Number	Impervious (%)	Time of Concentration (HR)	Storage Coefficient (HR)	Initial Type	Initial Discharge (M3/S)	Recession Constant	Threshold Type	Ratio to Peak
W1250	0.20723	94.5	0	22.9	3.559095	Discharge	0.1585	1	Ratio to Peak	0.5
W1260	0.207	94.5	0	22.9	1.724268	Discharge	0.0219633	1	Ratio to Peak	0.5
W1270	0.207	94.5	0	22.9	2.211969	Discharge	0.072943	1	Ratio to Peak	0.5
W1280	0.207	94.5	0	22.9	2.501135	Discharge	0.078203	1	Ratio to Peak	0.5
W1290	0.207	94.5	0	22.9	2.223681	Discharge	0.0575539	1	Ratio to Peak	0.5
W1300	0.177301	94.5	0	22.9	2.576987	Discharge	0.0793046	1	Ratio to Peak	0.5
W1310	0.207	94.5	0	22.9	3.829882	Discharge	0.11831	1	Ratio to Peak	0.5
W1320	0.20885	94.5	0	22.9	1.094694	Discharge	0.0055187	1	Ratio to Peak	0.5
W1330	0.198424	94.5	0	22.9	2.905052	Discharge	0.16873	1	Ratio to Peak	0.5
W1340	0.207	94.5	0	22.9	4.325983	Discharge	0.0936587	1	Ratio to Peak	0.5
W1350	0.199559	94.5	0	22.9	3.273026	Discharge	0.11208	1	Ratio to Peak	0.5

Basin Number	SCS Curve Number Loss			Clark Unit Hydrograph Transform		Recession Baseflow				
	Initial Abstraction (mm)	Curve Number	Impervious (%)	Time of Concentration (HR)	Storage Coefficient (HR)	Initial Type	Initial Discharge (M3/S)	Recession Constant	Threshold Type	Ratio to Peak
W1360	0.226499	94.5	0	22.9	2.602756	Discharge	0.0281327	1	Ratio to Peak	0.5
W1370	0.181839	94.5	0	22.9	3.251294	Discharge	0.0796417	1	Ratio to Peak	0.5
W1380	0.190479	94.5	0	22.9	4.189885	Discharge	0.14315	1	Ratio to Peak	0.5
W1390	0.207	94.5	0	22.9	2.316985	Discharge	0.0312282	1	Ratio to Peak	0.5
W1400	0.166818	94.5	0	22.9	3.104558	Discharge	0.16346	1	Ratio to Peak	0.5
W1410	0.208093	94.5	0	22.9	2.902722	Discharge	0.0363078	1	Ratio to Peak	0.5
W1420	0.207	94.5	0	22.9	3.502832	Discharge	0.11884	1	Ratio to Peak	0.5
W1430	0.197394	94.5	0	22.9	1.097137	Discharge	0.0141705	1	Ratio to Peak	0.5
W1440	0.207029	94.5	0	22.9	5.14167	Discharge	0.10635	1	Ratio to Peak	0.5
W1450	0.193632	94.5	0	22.9	0.46525	Discharge	0.00089438	1	Ratio to Peak	0.5
W1460	0.196695	94.5	0	22.9	3.613985	Discharge	0.15881	1	Ratio to Peak	0.5

Appendix

Basin Number	SCS Curve Number Loss			Clark Unit Hydrograph Transform		Recession Baseflow				
	Initial Abstraction (mm)	Curve Number	Impervious (%)	Time of Concentration (HR)	Storage Coefficient (HR)	Initial Type	Initial Discharge (M3/S)	Recession Constant	Threshold Type	Ratio to Peak
W1470	0.185026	94.5	0	22.9	2.901469	Discharge	0.0631252	1	Ratio to Peak	0.5
W1480	0.204643	94.5	0	22.9	2.142539	Discharge	0.0639562	1	Ratio to Peak	0.5
W1490	0.171431	94.5	0	22.9	3.41448	Discharge	0.14887	1	Ratio to Peak	0.5
W1500	0.202175	94.5	0	22.9	2.044894	Discharge	0.0365408	1	Ratio to Peak	0.5
W1510	0.202757	94.5	0	22.9	1.610156	Discharge	0.0170523	1	Ratio to Peak	0.5
W1520	0.207	94.5	0	22.9	1.885246	Discharge	0.0626592	1	Ratio to Peak	0.5
W1530	0.185179	94.5	0	22.9	0.966704	Discharge	0.0051011	1	Ratio to Peak	0.5
W1540	0.178708	94.5	0	22.9	3.141793	Discharge	0.19907	1	Ratio to Peak	0.5
W1550	0.188281	94.5	0	22.9	2.381561	Discharge	0.14628	1	Ratio to Peak	0.5
W1560	0.207	94.5	0	22.9	2.451315	Discharge	0.0753158	1	Ratio to Peak	0.5
W1570	0.190955	94.5	0	22.9	2.194047	Discharge	0.0477307	1	Ratio to Peak	0.5

Basin Number	SCS Curve Number Loss			Clark Unit Hydrograph Transform		Recession Baseflow				
	Initial Abstraction (mm)	Curve Number	Impervious (%)	Time of Concentration (HR)	Storage Coefficient (HR)	Initial Type	Initial Discharge (M3/S)	Recession Constant	Threshold Type	Ratio to Peak
W1580	0.184748	94.5	0	22.9	4.281642	Discharge	0.23133	1	Ratio to Peak	0.5
W1590	0.275	94.5	0	22.9	0.47752	Discharge		1	Ratio to Peak	0.5
W1600	0.208573	94.5	0	22.9	2.721681	Discharge	0.10748	1	Ratio to Peak	0.5
W1610	0.255828	94.5	0	22.9	7.77342	Discharge	0.26944	1	Ratio to Peak	0.5
W1620	0.070686	94.5	0	22.9	2.32636	Discharge	0.14879	1	Ratio to Peak	0.5
W1630	0.196227	94.5	0	22.9	1.813062	Discharge	0.079646	1	Ratio to Peak	0.5
W1640	0.197892	94.5	0	22.9	1.714646	Discharge	0.0559122	1	Ratio to Peak	0.5
W1650	0.174093	94.5	0	22.9	3.438112	Discharge	0.1227	1	Ratio to Peak	0.5
W1660	0.207123	94.5	0	22.9	5.755459	Discharge	0.27234	1	Ratio to Peak	0.5
W1670	0.049391	94.5	0	22.9	0.810535	Discharge	0.0087312	1	Ratio to Peak	0.5
W1680	0.083535	94.5	0	22.9	1.728307	Discharge	0.1315	1	Ratio to Peak	0.5

Basin Number	SCS Curve Number Loss			Clark Unit Hydrograph Transform		Recession Baseflow				
	Initial Abstraction (mm)	Curve Number	Impervious (%)	Time of Concentration (HR)	Storage Coefficient (HR)	Initial Type	Initial Discharge (M3/S)	Recession Constant	Threshold Type	Ratio to Peak
W1690	0.059238	94.5	0	22.9	2.626614	Discharge	0.15965	1	Ratio to Peak	0.5
W1700	0.185702	94.5	0	22.9	1.855547	Discharge	0.0575496	1	Ratio to Peak	0.5
W1710	0.193933	94.5	0	22.9	3.494681	Discharge	0.10991	1	Ratio to Peak	0.5
W1720	0.183342	94.5	0	22.9	5.239048	Discharge	0.22571	1	Ratio to Peak	0.5
W1730	0.239691	94.5	0	22.9	4.376547	Discharge	0.14089	1	Ratio to Peak	0.5
W1740	0.248386	94.5	0	22.9	4.129393	Discharge	0.13661	1	Ratio to Peak	0.5
W1750	0.135849	94.5	0	22.9	2.799012	Discharge	0.14146	1	Ratio to Peak	0.5
W1760	0.183591	94.5	0	22.9	2.211285	Discharge	0.0831484	1	Ratio to Peak	0.5
W1770	0.207	94.5	0	22.9	3.953835	Discharge	0.0826319	1	Ratio to Peak	0.5
W1780	0.207863	94.5	0	22.9	2.349459	Discharge	0.0647164	1	Ratio to Peak	0.5
W1790	0.196681	94.5	0	22.9	2.111076	Discharge	0.0432191	1	Ratio to Peak	0.5

Basin Number	SCS Curve Number Loss			Clark Unit Hydrograph Transform		Recession Baseflow				
	Initial Abstraction (mm)	Curve Number	Impervious (%)	Time of Concentration (HR)	Storage Coefficient (HR)	Initial Type	Initial Discharge (M3/S)	Recession Constant	Threshold Type	Ratio to Peak
W1800	0.071827	94.5	0	22.9	1.200796	Discharge	0.0558134	1	Ratio to Peak	0.5
W1810	0.075931	94.5	0	22.9	2.134583	Discharge	0.21503	1	Ratio to Peak	0.5
W1820	0.214769	94.5	0	22.9	0.899068	Discharge	0.009427	1	Ratio to Peak	0.5
W1830	0.067382	94.5	0	22.9	0.728286	Discharge	0.030453	1	Ratio to Peak	0.5
W1840	0.137298	94.5	0	22.9	2.679448	Discharge	0.12281	1	Ratio to Peak	0.5
W1850	0.226247	94.5	0	22.9	2.771673	Discharge	0.072083	1	Ratio to Peak	0.5
W1860	0.18455	94.5	0	22.9	2.004255	Discharge	0.058823	1	Ratio to Peak	0.5
W1870	0.077042	94.5	0	22.9	1.300863	Discharge	0.0633679	1	Ratio to Peak	0.5
W1880	0.264208	94.5	0	22.9	6.611858	Discharge	0.22347	1	Ratio to Peak	0.5
W1890	0.199119	94.5	0	22.9	3.064217	Discharge	0.11626	1	Ratio to Peak	0.5
W1900	0.154931	94.5	0	22.9	2.254287	Discharge	0.11987	1	Ratio to Peak	0.5

Appendix

Basin Number	SCS Curve Number Loss			Clark Unit Hydrograph Transform		Recession Baseflow				
	Initial Abstraction (mm)	Curve Number	Impervious (%)	Time of Concentration (HR)	Storage Coefficient (HR)	Initial Type	Initial Discharge (M3/S)	Recession Constant	Threshold Type	Ratio to Peak
W1910	0.27204	94.5	0	22.9	5.115754	Discharge	0.14602	1	Ratio to Peak	0.5
W1920	0.163899	94.5	0	22.9	4.276458	Discharge	0.15077	1	Ratio to Peak	0.5
W1930	0.1911	94.5	0	22.9	2.079611	Discharge	0.0674779	1	Ratio to Peak	0.5
W1940	0.196619	94.5	0	22.9	2.633001	Discharge	0.0922382	1	Ratio to Peak	0.5
W1950	0.198112	94.5	0	22.9	3.80935	Discharge	0.14734	1	Ratio to Peak	0.5
W1960	0.177198	94.5	0	22.9	2.161518	Discharge	0.0818181	1	Ratio to Peak	0.5
W1970	0.275	94.5	0	22.9	1.626447	Discharge	0.0050689	1	Ratio to Peak	0.5
W1980	0.275	94.5	0	22.9	4.639593	Discharge	0.069359	1	Ratio to Peak	0.5
W1990	0.275	94.5	0	22.9	2.049103	Discharge	0.0166292	1	Ratio to Peak	0.5
W2000	0.249276	94.5	0	22.9	2.342178	Discharge	0.0545626	1	Ratio to Peak	0.5
W2010	0.254017	94.5	0	22.9	4.864885	Discharge	0.12025	1	Ratio to Peak	0.5

Basin Number	SCS Curve Number Loss			Clark Unit Hydrograph Transform		Recession Baseflow				
	Initial Abstraction (mm)	Curve Number	Impervious (%)	Time of Concentration (HR)	Storage Coefficient (HR)	Initial Type	Initial Discharge (M3/S)	Recession Constant	Threshold Type	Ratio to Peak
W2020	0.163152	94.5	0	22.9	1.769427	Discharge	0.0350022	1	Ratio to Peak	0.5
W2030	0.204005	94.5	0	22.9	1.639683	Discharge	0.0588552	1	Ratio to Peak	0.5
W2040	0.220542	94.5	0	22.9	1.098929	Discharge	0.0145195	1	Ratio to Peak	0.5
W2050	0.163006	94.5	0	22.9	2.580668	Discharge	0.0689843	1	Ratio to Peak	0.5
W2060	0.250248	94.5	0	22.9	2.464008	Discharge	0.0576247	1	Ratio to Peak	0.5
W2070	0.275	94.5	0	22.9	1.450567	Discharge	0.0158766	1	Ratio to Peak	0.5
W2080	0.185336	94.5	0	22.9	2.108474	Discharge	0.0592696	1	Ratio to Peak	0.5
W2090	0.230561	94.5	0	22.9	2.842109	Discharge	0.0748456	1	Ratio to Peak	0.5
W2100	0.199393	94.5	0	22.9	2.846559	Discharge	0.0595595	1	Ratio to Peak	0.5
W2110	0.193049	94.5	0	22.9	3.514491	Discharge	0.0919344	1	Ratio to Peak	0.5
W2120	0.184338	94.5	0	22.9	2.44752	Discharge	0.0886961	1	Ratio to Peak	0.5

Basin Number	SCS Curve Number Loss			Clark Unit Hydrograph Transform		Recession Baseflow				
	Initial Abstraction (mm)	Curve Number	Impervious (%)	Time of Concentration (HR)	Storage Coefficient (HR)	Initial Type	Initial Discharge (M3/S)	Recession Constant	Threshold Type	Ratio to Peak
W2130	0.26667	94.5	0	22.9	5.104873	Discharge	0.13642	1	Ratio to Peak	0.5
W2140	0.219759	94.5	0	22.9	1.55857	Discharge	0.0196742	1	Ratio to Peak	0.5
W2150	0.122949	94.5	0	22.9	2.01804	Discharge	0.0954979	1	Ratio to Peak	0.5
W2160	0.256327	94.5	0	22.9	2.804915	Discharge	0.0612076	1	Ratio to Peak	0.5
W2170	0.275	94.5	0	22.9	3.00548	Discharge	0.0645124	1	Ratio to Peak	0.5
W2180	0.26511	94.5	0	22.9	2.503728	Discharge	0.0311326	1	Ratio to Peak	0.5
W2190	0.180623	94.5	0	22.9	3.540023	Discharge	0.1541	1	Ratio to Peak	0.5
W2200	0.209789	94.5	0	22.9	0.74201	Discharge	0.0043549	1	Ratio to Peak	0.5
W2210	0.199142	94.5	0	22.9	4.332259	Discharge	0.13952	1	Ratio to Peak	0.5
W2220	0.169	94.5	0	22.9	0.233237	Discharge	0.00025339	1	Ratio to Peak	0.5
W2230	0.195891	94.5	0	22.9	5.001114	Discharge	0.13397	1	Ratio to Peak	0.5

Basin Number	SCS Curve Number Loss			Clark Unit Hydrograph Transform		Recession Baseflow				
	Initial Abstraction (mm)	Curve Number	Impervious (%)	Time of Concentration (HR)	Storage Coefficient (HR)	Initial Type	Initial Discharge (M3/S)	Recession Constant	Threshold Type	Ratio to Peak
W2240	0.216898	94.5	0	22.9	5.520843	Discharge	0.17905	1	Ratio to Peak	0.5
W2250	0.255915	94.5	0	22.9	3.47337	Discharge	0.0888582	1	Ratio to Peak	0.5
W2260	0.275	94.5	0	22.9	9.495525	Discharge	0.1748	1	Ratio to Peak	0.5

Appendix B. Infanta Model Reach Parameters

Reach Number	Muskingum Cunge Channel Routing						
	Time Step Method	Length (m)	Slope	Man-ning's n	Shape	Width	Side Slope
R30	Automatic Fixed Interval	1698.4	0.004	0.01	Trapezoid	75	1
R50	Automatic Fixed Interval	1202.1	0.004	0.01	Trapezoid	75	1
R60	Automatic Fixed Interval	482.55	0.004	0.01	Trapezoid	75	1
R80	Automatic Fixed Interval	761.54	0.004	0.01	Trapezoid	75	1
R110	Automatic Fixed Interval	3868.4	0.004	0.01	Trapezoid	75	1
R140	Automatic Fixed Interval	1831.2	0.004	0.01	Trapezoid	75	1
R170	Automatic Fixed Interval	394.85	0.004	0.01	Trapezoid	75	1
R190	Automatic Fixed Interval	3951.7	0.004	0.01	Trapezoid	75	1
R200	Automatic Fixed Interval	1672.1	0.004	0.01	Trapezoid	75	1
R240	Automatic Fixed Interval	2919.1	0.004	0.01	Trapezoid	75	1
R250	Automatic Fixed Interval	5535	0.004	0.01	Trapezoid	75	1
R270	Automatic Fixed Interval	2875.2	0.004	0.01	Trapezoid	75	1
R280	Automatic Fixed Interval	4187.6	0.004	0.01	Trapezoid	75	1
R290	Automatic Fixed Interval	1412.7	0.004	0.01	Trapezoid	75	1
R300	Automatic Fixed Interval	476.98	0.004	0.01	Trapezoid	75	1
R360	Automatic Fixed Interval	1126.4	0.004	0.01	Trapezoid	75	1
R370	Automatic Fixed Interval	6935.7	0.004	0.01	Trapezoid	75	1
R380	Automatic Fixed Interval	2740.2	0.004	0.01	Trapezoid	75	1
R390	Automatic Fixed Interval	5483.3	0.004	0.01	Trapezoid	75	1
R400	Automatic Fixed Interval	2362.1	0.004	0.01	Trapezoid	75	1
R430	Automatic Fixed Interval	273.85	0.004	0.01	Trapezoid	75	1
R480	Automatic Fixed Interval	2721	0.004	0.01	Trapezoid	75	1
R490	Automatic Fixed Interval	1121.1	0.004	0.01	Trapezoid	75	1
R510	Automatic Fixed Interval	6911.7	0.004	0.01	Trapezoid	75	1
R530	Automatic Fixed Interval	5193.5	0.004	0.01	Trapezoid	75	1
R560	Automatic Fixed Interval	9074.8	0.004	0.01	Trapezoid	75	1
R590	Automatic Fixed Interval	10199	0.004	0.01	Trapezoid	75	1
R600	Automatic Fixed Interval	6590.7	0.004	0.01	Trapezoid	75	1
R630	Automatic Fixed Interval	6858.1	0.004	0.01	Trapezoid	75	1
R650	Automatic Fixed Interval	2836.5	0.004	0.01	Trapezoid	75	1
R670	Automatic Fixed Interval	5920	0.004	0.01	Trapezoid	75	1
R680	Automatic Fixed Interval	798.41	0.004	0.01	Trapezoid	75	1
R700	Automatic Fixed Interval	1971.1	0.004	0.01	Trapezoid	75	1
R710	Automatic Fixed Interval	6372	0.004	0.01	Trapezoid	75	1
R740	Automatic Fixed Interval	3154.6	0.004	0.01	Trapezoid	75	1

Reach Number	Muskingum Cunge Channel Routing						
	Time Step Method	Length (m)	Slope	Man-ning's n	Shape	Width	Side Slope
R750	Automatic Fixed Interval	3101.2	0.004	0.01	Trapezoid	75	1
R780	Automatic Fixed Interval	4409.7	0.004	0.01	Trapezoid	75	1
R790	Automatic Fixed Interval	8670	0.004	0.01	Trapezoid	75	1
R810	Automatic Fixed Interval	727.11	0.004	0.01	Trapezoid	75	1
R830	Automatic Fixed Interval	1141.2	0.004	0.01	Trapezoid	75	1
R840	Automatic Fixed Interval	2407.2	0.004	0.01	Trapezoid	75	1
R850	Automatic Fixed Interval	4540.3	0.004	0.01	Trapezoid	75	1
R880	Automatic Fixed Interval	2776.3	0.004	0.01	Trapezoid	75	1
R910	Automatic Fixed Interval	750.12	0.004	0.01	Trapezoid	75	1
R920	Automatic Fixed Interval	1169.4	0.004	0.01	Trapezoid	75	1
R930	Automatic Fixed Interval	4197.1	0.004	0.01	Trapezoid	75	1
R940	Automatic Fixed Interval	2524.8	0.004	0.01	Trapezoid	75	1
R960	Automatic Fixed Interval	4072.5	0.004	0.01	Trapezoid	75	1
R980	Automatic Fixed Interval	1707.8	0.004	0.01	Trapezoid	75	1
R1010	Automatic Fixed Interval	2679.7	0.004	0.01	Trapezoid	75	1
R1020	Automatic Fixed Interval	868.41	0.004	0.01	Trapezoid	75	1
R1030	Automatic Fixed Interval	1219.9	0.004	0.01	Trapezoid	75	1
R1050	Automatic Fixed Interval	3951.9	0.004	0.01	Trapezoid	75	1
R1060	Automatic Fixed Interval	165.56	0.004	0.01	Trapezoid	75	1
R1080	Automatic Fixed Interval	5546.7	0.004	0.01	Trapezoid	75	1
R1110	Automatic Fixed Interval	5943.2	0.004	0.01	Trapezoid	75	1

Appendix C. Infanta Discharge from HEC-HMS Simulation

DIRECT FLOW (cms)							
Time (hr)	100-yr	25-yr	5-year	Time (hr)	100-yr	25-yr	5-year
0	0	0	0	5.833333	0	0	0.1
0.166667	0	0	0	6	0	0	0.2
0.333333	0	0	0	6.166667	0	0	0.2
0.5	0	0	0	6.333333	0	0	0.4
0.666667	0	0	0	6.5	0	0	0.6
0.833333	0	0	0	6.666667	0	0	0.9
1	0	0	0	6.833333	0	0	1.2
1.166667	0	0	0	7	0	0.1	1.7
1.333333	0	0	0	7.166667	0.1	0.2	2.3
1.5	0	0	0	7.333333	0.2	0.3	3
1.666667	0	0	0	7.5	0.4	0.5	3.9
1.833333	0	0	0	7.666667	0.6	0.8	4.9
2	0	0	0	7.833333	1	1.2	6.2
2.166667	0	0	0	8	1.6	1.8	7.7
2.333333	0	0	0	8.166667	2.3	2.5	9.4
2.5	0	0	0	8.333333	3.3	3.4	11.4
2.666667	0	0	0	8.5	4.5	4.5	13.8
2.833333	0	0	0	8.666667	6	5.8	16.4
3	0	0	0	8.833333	7.8	7.5	19.4
3.166667	0	0	0	9	10	9.4	22.8
3.333333	0	0	0	9.166667	12.8	11.8	26.7
3.5	0	0	0	9.333333	16.4	14.9	31.3
3.666667	0	0	0	9.5	20.9	18.5	36.5
3.833333	0	0	0	9.666667	26.4	23	42.4
4	0	0	0	9.833333	33.3	28.5	49.3
4.166667	0	0	0	10	41.6	35.1	57.1
4.333333	0	0	0	10.16667	51.7	42.9	65.9
4.5	0	0	0	10.33333	63.5	52	75.8
4.666667	0	0	0	10.5	77.5	62.7	86.9
4.833333	0	0	0	10.66667	93.9	75.2	99.3
5	0	0	0	10.83333	113	89.6	113.3
5.166667	0	0	0	11	135	106.1	128.8
5.333333	0	0	0	11.16667	161.5	125.8	146.4
5.5	0	0	0	11.33333	193.1	149.1	166.2
5.666667	0	0	0.1	11.5	229.9	176.1	188.4

DIRECT FLOW (cms)							
Time (hr)	100-yr	25-yr	5-year	Time (hr)	100-yr	25-yr	5-year
11.66667	274.1	208.7	213.7	18	8237.5	6255.6	4347.4
11.83333	337.9	256	243.3	18.16667	8278.1	6289.7	4388.8
12	416.3	314.4	281.5	18.33333	8304.9	6313.6	4421.3
12.16667	503.7	379.5	325.4	18.5	8317.7	6326.9	4445.9
12.33333	605.7	455.6	374.2	18.66667	8301.2	6318.1	4462
12.5	732	550	430.7	18.83333	8260.6	6290.7	4464.3
12.66667	873.7	656.3	497.3	19	8207.2	6253.6	4456.1
12.83333	1025.1	769.7	570.7	19.16667	8142.2	6207.9	4440.8
13	1191	894.1	649.6	19.33333	8062.2	6151	4418.7
13.16667	1373	1030.5	735.8	19.5	7971	6085.8	4389.6
13.33333	1565.7	1175	829.1	19.66667	7871.9	6014.6	4354.8
13.5	1767.8	1326.6	928	19.83333	7762.9	5936.1	4314.6
13.66667	1989.3	1492.8	1032.7	20	7642.6	5849	4268.8
13.83333	2227.7	1672	1146.3	20.16667	7513.4	5755.2	4217.4
14	2476.5	1859	1267.1	20.33333	7376.8	5655.9	4161.4
14.16667	2736.3	2054.5	1393.4	20.5	7227.6	5547.1	4100.8
14.33333	3021.1	2269.1	1525.8	20.66667	7065.5	5428.4	4034.2
14.5	3322.2	2496.5	1668.8	20.83333	6894.7	5303.1	3962.3
14.66667	3630.6	2729.5	1818.3	21	6716.5	5172.1	3886.4
14.83333	3949.1	2970.6	1972	21.16667	6525.8	5031.6	3806.9
15	4282.2	3223	2131.1	21.33333	6325.7	4883.6	3721.6
15.16667	4621.5	3480.8	2296.3	21.5	6122.1	4732.8	3632.4
15.33333	4960.9	3738.9	2464.7	21.66667	5917.9	4581.7	3541
15.5	5292	3990.8	2633.5	21.83333	5720.3	4435.4	3448.9
15.66667	5610.4	4233.3	2798.9	22	5527.1	4292.6	3359.3
15.83333	5920.5	4469.6	2959.9	22.16667	5335.7	4151.2	3270.4
16	6222.3	4699.9	3118	22.33333	5151.4	4015	3182.1
16.16667	6498.7	4911.2	3271.4	22.5	4979.2	3888.1	3097.1
16.33333	6752.9	5105.6	3413.9	22.66667	4813.3	3766.2	3016.6
16.5	6994.9	5291	3548.2	22.83333	4650.3	3646.4	2938.3
16.66667	7222.6	5465.7	3676.4	23	4493	3530.8	2861.6
16.83333	7418	5616.3	3796.8	23.16667	4341.2	3419.2	2787.6
17	7592.3	5750.5	3903.5	23.33333	4192.6	3310.1	2715.9
17.16667	7753.8	5875.4	4001.2	23.5	4047.1	3203.2	2645.9
17.33333	7894.8	5984.9	4091.7	23.66667	3908.2	3101.2	2577.5
17.5	8005.8	6071.7	4171.9	23.83333	3774.2	3002.9	2511.9
17.66667	8098	6144.1	4239	24	3643.6	2907	2448.4
17.83333	8177.4	6206.9	4297	24.16667	3517.5	2814.4	2386.5

DIRECT FLOW (cms)							
Time (hr)	100-yr	25-yr	5-year	Time (hr)	100-yr	25-yr	5-year
24.33333	3399.4	2727.8	2326.5	30.66667	814.3	718.8	742.5
24.5	3286.9	2645.3	2269.8	30.83333	781.4	690.2	713.6
24.66667	3177.3	2564.9	2215.2	31	749.4	662.3	685.4
24.83333	3070.7	2486.5	2161.9	31.16667	718.5	635.3	658.1
25	2966.9	2410	2109.9	31.33333	688.6	609	631.4
25.16667	2865.4	2335	2058.8	31.5	659.4	583.5	605.4
25.33333	2765.8	2261.3	2008.8	31.66667	631.4	558.8	580.1
25.5	2669.8	2190	1959.9	31.83333	604.9	535.4	555.6
25.66667	2577.4	2121.4	1912.4	32	579.6	513	532.1
25.83333	2487.2	2054.1	1866	32.16667	555.1	491.3	509.5
26	2398.7	1988	1820.2	32.33333	531.5	470.3	487.6
26.16667	2312.3	1923.1	1774.8	32.5	508.8	450.1	466.5
26.33333	2227.9	1859.4	1729.5	32.66667	486.7	430.5	446.1
26.5	2145.4	1796.8	1684.4	32.83333	465.4	411.6	426.5
26.66667	2065.7	1736.1	1639.7	33	445.4	393.7	407.7
26.83333	1991.5	1679.2	1595.6	33.16667	426.5	376.9	389.9
27	1920.9	1624.9	1553.2	33.33333	408.4	360.9	373.1
27.16667	1852.2	1571.7	1511.3	33.5	391.1	345.5	357.1
27.33333	1785.4	1519.7	1469.8	33.66667	374.4	330.7	341.8
27.5	1720.7	1468.8	1428.5	33.83333	358.4	316.5	327.2
27.66667	1657.4	1418.8	1387.3	34	342.9	302.9	313.2
27.83333	1595.6	1369.6	1346.3	34.16667	328.2	289.9	299.9
28	1536.9	1322.6	1305.8	34.33333	314.3	277.6	287.1
28.16667	1481	1277.5	1266.2	34.5	301.1	266	275
28.33333	1426.5	1233.4	1227.3	34.66667	288.3	254.7	263.4
28.5	1373.2	1189.9	1188.9	34.83333	276.1	243.9	252.3
28.66667	1321.4	1147.4	1151	35	264.3	233.5	241.6
28.83333	1270.8	1105.7	1113.4	35.16667	252.9	223.5	231.4
29	1221.3	1064.7	1076.2	35.33333	242	213.9	221.5
29.16667	1173.5	1024.9	1039.3	35.5	231.8	204.8	212.1
29.33333	1128.4	987	1003.3	35.66667	222.2	196.4	203.2
29.5	1085.1	950.6	968.4	35.83333	213.1	188.3	194.7
29.66667	1042.9	914.9	934.3	36	204.3	180.5	186.7
29.83333	1001.7	879.9	900.8	36.16667	195.9	173	178.9
30	961.7	845.8	867.9	36.33333	187.7	165.8	171.4
30.16667	922.6	812.3	835.5	36.5	179.9	158.8	164.1
30.33333	884.5	779.6	803.6	36.66667	172.4	152.2	157.2
30.5	848.4	748.4	772.5	36.83333	165.5	146.1	150.6

DIRECT FLOW (cms)							
Time (hr)	**100-yr**	**25-yr**	**5-year**	**Time (hr)**	**100-yr**	**25-yr**	**5-year**
37	159	140.3	144.4	43.33333	16.5	16.3	20.7
37.16667	152.8	134.7	138.4	43.5	15.3	15.3	19.5
37.33333	146.8	129.3	132.7	43.66667	14.3	14.3	18.4
37.5	141	124.2	127.3	43.83333	13.3	13.4	17.3
37.66667	135.4	119.2	122	44	12.4	12.6	16.3
37.83333	129.9	114.3	116.9	44.16667	11.6	11.8	15.4
38	124.7	109.7	112.1	44.33333	10.8	11.1	14.6
38.16667	119.6	105.2	107.4	44.5	10.1	10.4	13.7
38.33333	114.6	100.8	102.9	44.66667	9.4	9.8	13
38.5	109.8	96.6	98.7	44.83333	8.7	9.2	12.3
38.66667	105.1	92.5	94.5	45	8.1	8.6	11.6
38.83333	100.5	88.4	90.5	45.16667	7.6	8.1	10.9
39	96.1	84.5	86.6	45.33333	7	7.6	10.3
39.16667	91.7	80.7	82.8	45.5	6.6	7.1	9.8
39.33333	87.5	77.1	79.1	45.66667	6.2	6.7	9.2
39.5	83.3	73.5	75.6	45.83333	5.8	6.3	8.7
39.66667	79.3	70	72.2	46	5.4	5.9	8.3
39.83333	75.4	66.6	68.9	46.16667	5	5.6	7.8
40	71.7	63.4	65.7	46.33333	4.7	5.2	7.4
40.16667	68.1	60.3	62.6	46.5	4.4	4.9	7
40.33333	64.5	57.2	59.7	46.66667	4.1	4.6	6.6
40.5	61	54.2	56.8	46.83333	3.8	4.3	6.3
40.66667	57.7	51.4	54	47	3.5	4	5.9
40.83333	54.4	48.5	51.3	47.16667	3.3	3.8	5.6
41	51.2	45.8	48.7	47.33333	3	3.6	5.3
41.16667	48	43.1	46.2	47.5	2.8	3.3	5
41.33333	45	40.5	43.8	47.66667	2.6	3.1	4.7
41.5	42	38	41.4				
41.66667	39	35.5	39.1				
41.83333	36.2	33.1	36.9				
42	33.4	30.7	34.7				
42.16667	30.7	28.4	32.6				
42.33333	28.1	26.3	30.6				
42.5	25.6	24.1	28.7				
42.66667	23.2	22.1	26.8				
42.83333	21	20.2	25.1				
43	19.2	18.7	23.4				
43.16667	17.8	17.4	22				

D R E A M

Disaster RIsk and Exposure Assessment for Mitigation